Combined immunodeficiency and Epstein-Barr virus–induced B cell malignancy in humans with inherited CD70 deficiency

Hassan Abolhassani,[1,3]* Emily S.J. Edwards,[4,5]* Aydan Ikinciogullari,[6]* Huie Jing,[8,9]* Stephan Borte,[12] Marcus Buggert,[2,13] Likun Du,[1] Mami Matsuda-Lennikov,[9,10] Rosa Romano,[1] Rozina Caridha,[1] Sangeeta Bade,[8,9] Yu Zhang,[8,9] Juliet Frederiksen,[14] Mingyan Fang,[1] Sevgi Kostel Bal,[6] Sule Haskologlu,[6] Figen Dogu,[6] Nurdan Tacyildiz,[7] Helen F. Matthews,[8,9,10] Joshua J. McElwee,[15] Emma Gostick,[16] David A. Price,[11,16] Umaimainthan Palendira,[17] Asghar Aghamohammadi,[3,18] Bertrand Boisson,[19,20,22] Nima Rezaei,[3,18] Annika C. Karlsson,[2] Michael J. Lenardo,[9,10] Jean-Laurent Casanova,[19,20,21,22,23] Lennart Hammarström,[1] Stuart G. Tangye,[4,5]** Helen C. Su,[8,9]** and Qiang Pan-Hammarström[1]**

[1]Division of Clinical Immunology and [2]Division of Clinical Microbiology, Department of Laboratory Medicine, Karolinska Institutet at Karolinska University Hospital Huddinge, SE1418 Stockholm, Sweden
[3]Research Center for Immunodeficiencies, Children's Medical Center, Tehran University of Medical Sciences, 14149 Tehran, Iran
[4]Immunology Division, Garvan Institute of Medical Research, Darlinghurst NSW 2010, Australia
[5]St. Vincent's Clinical School, Faculty of Medicine, University of New South Wales, Darlinghurst NSW 2010, Australia
[6]Department of Pediatric Immunology and Allergy and [7]Department of Pediatric Hematology and Oncology, Ankara University Medical School, 06100 Dikimevi-Ankara, Turkey
[8]Laboratory of Host Defenses, [9]Clinical Genomics Program, [10]Laboratory of Immunology, and [11]Vaccine Research Center, National Institute of Allergy and Infectious Diseases, National Institutes of Health, Bethesda, MD 20892
[12]ImmunoDeficiency Center Leipzig, Hospital St. Georg Leipzig, D-04129 Leipzig, Germany
[13]Department of Microbiology, University of Pennsylvania, Philadelphia, PA 19104
[14]Department of Systems Biology, Technical University of Denmark, 2800 Kgs. Lyngby, Denmark
[15]Merck Research Laboratories, Merck & Co., Boston, MA 02115
[16]Division of Infection and Immunity, Cardiff University School of Medicine, Cardiff CF14 4XN, Wales, UK
[17]Centenary Institute, University of Sydney, Newtown NSW 2042, Australia
[18]Primary Immunodeficiency Diseases Network, Universal Scientific Education and Research Network, 14149 Tehran, Iran
[19]St. Giles Laboratory of Human Genetics of Infectious Diseases, The Rockefeller University, New York, NY 10065
[20]Laboratory of Human Genetics of Infectious Diseases, Institut National de la Santé et de la Recherche Médicale U.1163 and [21]Pediatric Hematology-Immunology Unit, Necker Hospital for Sick Children, 75015 Paris, France
[22]Paris Descartes University, Imagine Institute, 75015 Paris, France
[23]Howard Hughes Medical Institute, New York, NY 10065

In this study, we describe four patients from two unrelated families of different ethnicities with a primary immunodeficiency, predominantly manifesting as susceptibility to Epstein-Barr virus (EBV)–related diseases. Three patients presented with EBV-associated Hodgkin's lymphoma and hypogammaglobulinemia; one also had severe varicella infection. The fourth had viral encephalitis during infancy. Homozygous frameshift or in-frame deletions in *CD70* in these patients abolished either CD70 surface expression or binding to its cognate receptor CD27. Blood lymphocyte numbers were normal, but the proportions of memory B cells and EBV-specific effector memory CD8$^+$ T cells were reduced. Furthermore, although T cell proliferation was normal, in vitro–generated EBV-specific cytotoxic T cell activity was reduced because of CD70 deficiency. This reflected impaired activation by, rather than effects during killing of, EBV-transformed B cells. Notably, expression of 2B4 and NKG2D, receptors implicated in controlling EBV infection, on memory CD8$^+$ T cells from CD70-deficient individuals was reduced, consistent with their impaired killing of EBV-infected cells. Thus, autosomal recessive CD70 deficiency is a novel cause of combined immunodeficiency and EBV-associated diseases, reminiscent of inherited CD27 deficiency. Overall, human CD70–CD27 interactions therefore play a nonredundant role in T and B cell–mediated immunity, especially for protection against EBV and humoral immunity.

*H. Abolhassani, E.S.J. Edwards, A. Ikinciogullari, and H. Jing contributed equally to this paper.

**S.G. Tangye, H.C. Su, and Q. Pan-Hammarström contributed equally to this paper.

Correspondence to Qiang Pan-Hammarström: Qiang.Pan-Hammarstrom@ki.se; Stuart G. Tangye: s.tangye@garvan.org.au; or Helen C. Su: hsu@niaid.nih.gov

Abbreviations used: EBNA, EBV nuclear antigen; HL, Hodgkin's lymphoma; IVIG, intravenous IgG; LCL, lymphoblastoid cell line; PID, primary immunodeficiency; rhIL, recombinant human IL; VCA, viral capsid antigen; WES, whole-exome sequencing; WGS, whole-genome sequencing; XLP, X-linked lymphoproliferative.

© 2017 Abolhassani et al. This article is distributed under the terms of an Attribution–Noncommercial–Share Alike–No Mirror Sites license for the first six months after the publication date (see http://www.rupress.org/terms/). After six months it is available under a Creative Commons License (Attribution–Noncommercial–Share Alike 4.0 International license, as described at https://creativecommons.org/licenses/by-nc-sa/4.0/).

The Rockefeller University Press $30.00
J. Exp. Med. 2017 Vol. 214 No. 1 91–106
https://doi.org/10.1084/jem.20160849

The Journal of Experimental Medicine

Downloaded from http://rupress.org/jem/article-pdf/214/1/91/1133722/jem_20160849.pdf by Ankara Universitesi Fen user on 11 December 2021

INTRODUCTION

Nearly 300 types of inborn errors of immunity, mainly caused by mutations in single genes, have been recognized to date (Picard et al., 2015). These primary immunodeficiencies (PIDs) predispose affected individuals to infections, autoinflammation, autoimmunity, allergy, and malignancy. The severity of PIDs ranges from life-threatening manifestations in early childhood to milder defects with later onset. Prototypic PIDs are typically monogenic but do not necessarily display complete clinical penetrance, as genetically affected relatives of index cases may be asymptomatic. In addition, several phenotypes can be allelic at the same locus, allowing the clinical presentation of any given inborn error to vary greatly between individuals. Although the first-described PIDs were associated with multiple, recurrent, opportunistic infections, not all PIDs are characterized by severe infectious diseases. Among those associated with severe infections, susceptibility can be global (i.e., to a wide variety of pathogens) or restricted to a small number of microorganisms, sometimes even a single pathogen, for instance EBV (Casanova, 2015a,b).

Primary infection with EBV, one of eight known human herpes viruses, typically occurs in childhood and is usually asymptomatic but can cause self-limiting infectious mononucleosis during adolescence or adulthood (Taylor et al., 2015). Severe EBV-associated diseases are seen in patients with three nonmutually exclusive groups of PIDs: those with broad defects in T cell immunity, familial forms of lymphohistiocytosis, and disorders of DNA repair (Faitelson and Grunebaum, 2014; Palendira and Rickinson, 2015; Taylor et al., 2015). In most of these conditions, EBV is only one of many microbial threats. However, selective susceptibility to EBV-induced diseases is the main characteristic of patients suffering from X-linked lymphoproliferative (XLP) syndrome caused by mutations in *SH2D1A* (Tangye, 2014) or *BIRC4* (Aguilar and Latour, 2015). Affected males develop hemophagocytic lymphohistiocytosis, hypogammaglobulinemia, and/or lymphoid malignancy. Patients with mutations in *ITK*, *MAGT1*, *CORO1A*, *FCGR3A*, or *CD27* are also vulnerable to EBV and occasionally other herpes viruses (Cohen, 2015; Taylor et al., 2015).

CD27, a TNF receptor superfamily member, is expressed on human naive and some memory T cells, germinal center and memory B cells, plasma cells, and a subset of NK cells (Tangye et al., 1998; Jung et al., 2000; Borst et al., 2005; Silva et al., 2008; Vossen et al., 2008). Its specific ligand, CD70, a cytokine structurally related to TNF, is only transiently expressed on activated dendritic, T, and B cells (Lens et al., 1996; Tesselaar et al., 2003; Borst et al., 2005). Studies of mouse and human immune cells have implicated CD70–CD27 interaction in T cell expansion and survival, germinal center formation, B cell activation and antibody production, and NK cell function (Hintzen et al., 1995; Jacquot et al., 1997; Agematsu et al., 1998; Borst et al., 2005; Nolte et al., 2009; De Colvenaer et al., 2011). Currently, 16 individuals with confirmed and one patient with potential biallelic-null mutations in *CD27* have been reported (van Montfrans et al., 2012; Salzer et al., 2013; Alkhairy et al., 2015a). They display EBV-associated lymphoproliferative disease, lymphoma, and/or hypogammaglobulinemia. Here, we describe four patients from two unrelated and ethnically distinct families with autosomal recessive CD70 deficiency causing a similar clinical phenotype.

RESULTS

Four affected individuals from two unrelated consanguineous families with viral infections and EBV-associated malignancy

The proband from family 1 (P1) is a female born to Persian consanguineous parents. At 5 yr of age, she had severe chickenpox infection with varicella pneumonia. At age 8, she suffered from Behçet's-like syndrome, with nonerosive oligoarthritis, oral aphthous ulcers, and posterior uveitis. At age 9, she had recurrent upper respiratory tract infections, hypogammaglobulinemia, and poor antibody responses to tetanus and diphtheria vaccinations but normal T and B cell numbers (Table 1 and Fig. S1). Intravenous IgG (IVIG) replacement and prophylactic treatment with antibiotics reduced the frequency and severity of infections. She subsequently developed finger clubbing, mild restrictive and obstructive pulmonary function, alopecia areata, peptic ulcer and gastritis, splenomegaly, and lymphadenopathy. At age 17, a gastric biopsy from an ulcerated lesion revealed mixed cellularity–type Hodgkin's lymphoma (HL) with strong expression of EBV nuclear antigen 1 (EBNA1). She achieved clinical remission after four cycles of chemotherapy. P1 has three healthy siblings; however, a fourth sibling (P2, IV.3; Fig. 1 A) had encephalitis during infancy caused by an undefined central nervous system viral infection. Normal lymphocyte counts (Fig. S1) and serum Ig levels but low postvaccination antibody titers against tetanus and diphtheria were observed (Table S1). Anti-EBV, CMV, HSV-1, and varicella-zoster IgG were present at high titers in P1 and P2 (Table 1 and Table S1), but neither EBV nor CMV were detected in plasma by PCR, suggesting disease remission. At the most recent follow up, P1 (age 29) was clinically stable on monthly IVIG and prophylactic antimicrobial therapy; P2 (age 33) was intellectually disabled but did not present with other clinical manifestations. The parents have no signs of immunodeficiency, but the father developed prostate cancer at the age of 53, and the mother was diagnosed with uterine cancer and astrocytoma at 53 and 60 yr of age, respectively (Fig. 1 A). The mother also had two unexplained miscarriages. Both maternal and paternal grandparents died from malignancies (II.1-II.4; Fig. 1 A).

The proband from family 2 (P3), of Turkish consanguineous origin, had recurrent otitis media, frequent fever, and diarrhea starting at 1 yr of age. At 2.5 yr of age, he developed diffuse cervical lymphadenopathy. Excisional biopsy revealed mixed cellularity–type HL that was positive for EBV-latent membrane protein 1. EBV viral capsid antigen (VCA) IgG was positive, and EBV DNA was detected in the blood. Ig

Downloaded from http://rupress.org/jem/article-pdf/214/1/91/1133722/jem_20160849.pdf by Ankara Universitesi Fen user on 11 December 2021

levels were reduced, but specific antibody responses were present (Table 1). Peripheral lymphocyte immunophenotyping was normal except for a transient $CD4^+$ T cell lymphopenia (Fig. S1). Although remission was achieved with six cycles of chemotherapy, relapse of HL occurred in the same region. Additional chemo/radiotherapy resulted in complete remission. As Ig levels remained low, IVIG and antimicrobial prophylaxis were started. After 9 yr of an uneventful clinical course, he had elevated EBV PCR copy numbers, which were responsive to rituximab treatment. He currently remains in complete remission at age 16. P3 has a brother (P4; Fig. 1 B) who was almost 3 yr old when he developed chronic cervical lymphadenopathy with an EBV-associated mixed cellular HL. Serum EBV VCA IgG was positive, and EBV was also detected by PCR in his cerebrospinal fluid. He showed normal lymphocyte immunophenotyping but a history of recurrent upper respiratory tract infections and hypogammaglobulinemia (Table 1 and Fig. S1), for which IVIG and antimicrobial prophylaxis were given. Although he entered remission after six cycles of chemotherapy, HL relapsed 2 yr later. Chemotherapy was followed by autologous hematopoietic stem cell transplantation. Although he had an episode of posttransplant EBV flare up, he currently remains in complete remission (at age 8). The parents have no immunodeficiency, but the mother had breast cancer at the age of 35.

Homozygous frameshift or in-frame deletions in CD70 in the four affected individuals

In family 1, whole-exome sequencing (WES) was performed for the index patient P1. As she was born to consanguineous parents, an autosomal recessive pattern of inheritance was expected; nonsynonymous rare variations (minor allele frequency <1%) in a homozygous status were thus prioritized. Mutations in known PID genes (Picard et al., 2015) were not observed. However, a novel homozygous 1-bp deletion in exon 3 of *CD70* (c.250delT), predicted to change the reading frame at amino acid 84 and create a premature stop codon 27 amino acids downstream of the mutation (p.S84Pfs27X), was detected. WES was also performed for P2, and the *CD70* mutation was the only candidate among the shared homozygous variants that could explain the immunodeficiency observed in both siblings. Sanger sequencing confirmed that the two siblings were homozygous and the parents and healthy siblings were heterozygous for this mutation (Fig. 1 C). This mutation was not found in the 1000 Genomes, National Heart, Lung, and Blood Institute exome sequencing project, and Exome Aggregation Consortium databases or in 251 Iranian blood donors and our recent study of the Middle Eastern Variome (Scott et al., 2016). The mutation is predicted to be deleterious (for details, see the Genetic analysis section of Materials and methods).

In family 2, whole-genome sequencing (WGS) was performed on the affected sibling (P4) and both parents. We used a similar strategy to family 1 for filtering and prioritizing variants and identified a novel homozygous 3-bp deletion (c.555_557delCTT), also located in exon 3 of *CD70*, predicted to be deleterious and cause an in-frame deletion at position 186 (p.F186del). Sanger sequencing identified the same homozygous *CD70* mutation in the proband (P3) and confirmed the homozygous mutation status in P4 and the heterozygous status of both parents (Fig. 1 D).

Lack of expression or altered binding of the mutant CD70 protein

Quantitative PCR demonstrated normal *CD70* mRNA levels in PBMCs from the two affected siblings in family 1, indicating minimal nonsense-mediated mRNA decay (not depicted). Flow cytometric analysis showed that CD70 was absent from B cells from P1 or P2, and expression was reduced to ∼50% of the normal value in the heterozygous father (Fig. 2 A). Western blotting of HEK293 cells transfected with WT or mutant (p.S84Pfs27X) CD70 was performed

Table 1. **Serum Ig levels in CD70-deficient patients**

Parameters	Age of P1			Age of P2	Age of P3		Age of P4	
	9 yr	17 yr	26 yr	30 yr	2.5 yr	5 yr	2.8 yr	8 yr
Diagnosis	CVID dx	HL dx	Genetic dx	Genetic dx	HL dx	Genetic dx	HL dx	Genetic dx
IgG, mg/dl	**389↓** (600–1,500)	**439↓**[a] (600–1,500)	843[a] (600–1,500)	1,080 (600–1,500)	**315↓** (640–2,010)	**323↓**[a] (640–2,010)	**462↓** (640–2,010)	**403↓** (764–2,134)
IgA, mg/dl	**76↓** (80–380)	**<10↓** (80–380)	**67↓** (80–380)	262 (80–380)	**6.7↓** (44–244)	**<10↓** (50–266)	27 (26–296)	**26↓** (70–303)
IgM, mg/dl	**48↓** (50–370)	**<20↓** (50–370)	**16↓** (50–370)	56 (50–370)	**18↓** (52–297)	**<19↓** (51–373)	**52↓** (71–235)	**36↓** (69–387)
IgE, IU/ml	3 (0–10)	2 (0–10)	3 (0–10)	4 (0–10)	NA	NA	NA	NA
Antidiphtheria IgG, IU/ml	**<0.01↓**[b] (>0.01)	NA	0.2[a] (>0.01)	**≤0.006↓**[c] (>0.01)	NA	NA	NA	NA
Antitetanus IgG, IU/ml	**<0.01↓**[b] (>0.05)	NA	1.04[a] (>0.05)	**0.03↓**[c] (>0.05)	NA	NA	NA	NA
Antirubella IgG	NA	NA	NA	NA	NA	NA	Positive	NA
Anti-CMV IgG	NA	NA	Positive[a]	Positive	Positive	NA	Negative	NA
Anti-EBV VCA IgG	NA	NA	Positive[a]	Positive	Positive	NA	Positive	NA

Numbers in parentheses indicate reference range. CVID, common variable immune deficiency; Dx, diagnosis; NA, not available.
[a]After commencing IVIG therapy.
[b]Vaccinated with diphtheria, pertussis, tetanus triple vaccine at age 6 yr.
[c]Vaccinated with tetanus-diphtheria adult booster vaccine at age 25 yr.

Downloaded from http://rupress.org/jem/article-pdf/214/1/91/1133722/jem_20160849.pdf by Ankara Universitesi Fen user on 11 December 2021

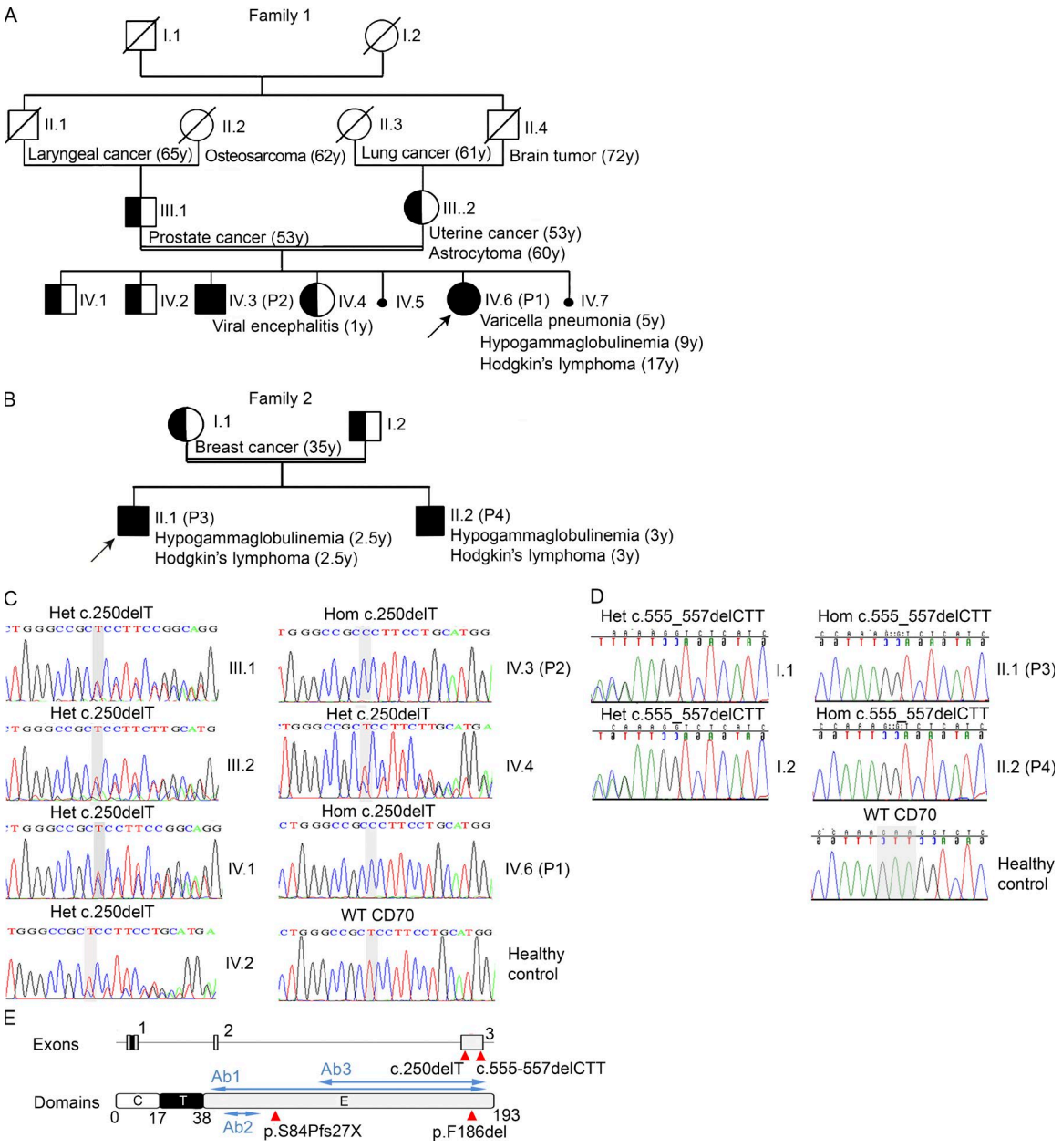

Figure 1. **Identification of *CD70* mutations in two families with immunodeficiency and malignancy.** (A) Family 1 pedigree. Cancer type, age of cancer diagnosis, and other key clinical manifestations in family members as well as the proband are shown. (B) Family 2 pedigree. Key clinical manifestations are shown. (A and B) /, deceased; double line, consanguinity; arrow, the proband (IV.6 in family 1 and II.1 in family 2); half-shaded, heterozygous; shaded, homozygous; unshaded, unknown; IV.5 and IV.7, miscarried fetus. (C) Sanger sequencing analysis of the *CD70* gene in family 1. A homozygous (Hom) mutation was confirmed in the proband (P1) and the affected sibling (P2; IV.3). Heterozygous (Het) mutations were identified in the parents and three healthy siblings. (D) Sanger sequencing analysis of the *CD70* gene in family 2. A homozygous mutation was confirmed in the proband (P3) and the affected sibling (P4). Heterozygous mutations were identified in the parents. Gray shading on the WT sequence indicates the bases that are deleted in the familial mutation. The sequences in this figure are in reverse direction. (C and D) The Sanger sequencing presented has been confirmed in at least two independent experiments. (E) The location of the mutation identified in the families in relation to the exon and protein domains (red triangles). The locations of antibodies (Ab1 recognizing amino acids 45–193, Ab2 recognizing amino acids 61–75, and Ab3 recognizing amino acids 129–193) used to detect CD70 protein expression are marked by blue arrows. C, cytoplasmic; E, extracellular; T, transmembrane.

Downloaded from http://rupress.org/jem/article-pdf/214/1/91/1133722/jem_20160849.pdf by Ankara Universitesi Fen user on 11 December 2021

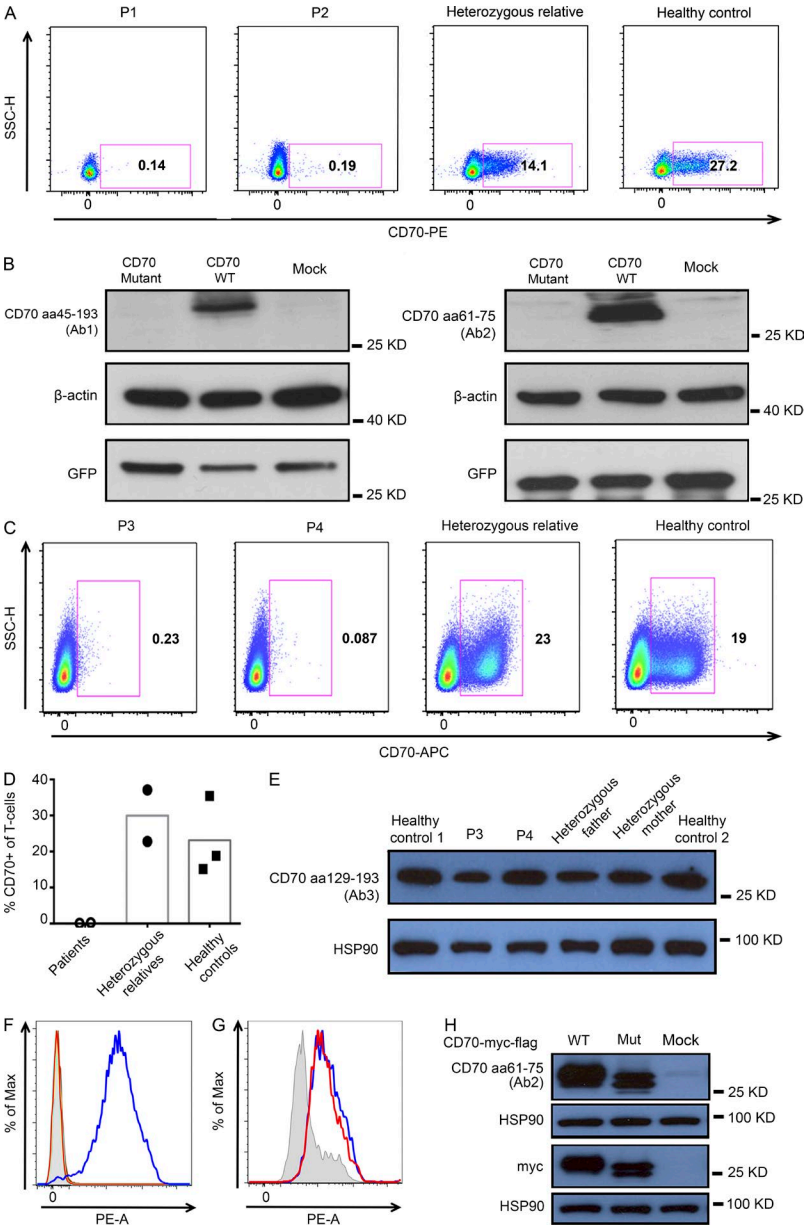

Figure 2. **Expression analysis of the CD70 mutants.** (A) Expression of CD70 by peripheral blood B cells from the CD70-deficient patients (P1 and P2), compared with a heterozygous relative (father) and a normal control. CD70 expression was analyzed on $CD19^+$-gated, live, single B cells. (B) Immunoblotting analysis of CD70 WT and mutant (identified in family 1) transfected HEK 293 cells. CD70 expression was probed with two different Abs specific for different epitopes (Ab1 and Ab2). GFP expression confirmed successful transfection, and β-actin served as a loading control. (C–E) Expression of CD70 by activated peripheral blood T cells from the two homozygous CD70-mutant patients (P3 and P4), compared with heterozygous parents (n = 2) and normal controls (n = 3). CD70 expression was analyzed by flow cytometry on $CD3^+$ gated, live, single T cells using a mAb raised against CD70-transfected L cells (C and D) or by immunoblotting using polyclonal Abs (Ab3) raised against an extended C-terminal portion of CD70 (E). HSP90 was used to assess protein loading. (F) Binding of overexpressed WT or mutant CD70 to recombinant human CD27 was evaluated by flow cytometry. Shaded areas represent nontransfected 293T cells. Binding of anti-CD5 mAbs to cells transfected with WT (turquoise) or mutant (yellow) CD70 is shown. Binding of biotinylated CD27/streptavidin-PE in cells transfected with WT (blue) or mutant (red) CD70 is shown. (G) Flow cytometric detection of the flag epitope on cells transfected with WT (blue) or mutant (red) CD70 or on untransfected cells (shaded). (H) Immunoblotting of lysates from untransfected cells or cells transfected with WT or mutant CD70 plasmid, using Abs to CD70 (Ab2), myc tag, or HSP90. All data are representative of at least two independent experiments. Mut, mutant; SSC, side scatter.

using two different antibodies recognizing distinct epitopes of CD70 (Ab1 and Ab2; Fig. 1 E and Fig. 2 B). Neither full-length nor truncated forms of mutant CD70 were detected, confirming that the patients' *CD70* allele is a loss-of-expression variant (Fig. 2 B).

In family 2, the *CD70* mutation caused the loss of the first of two phenylalanines, nine amino acids distant from the C terminus. This residue is predicted to contribute to a β-strand conserved among the TNF superfamily to which CD70 belongs (Goodwin et al., 1993; Tesselaar et al., 1997). To test the effect of this mutation on the structure and function of CD70, we first assessed CD70 expression. Using a mAb against the extracellular C-terminal portion of CD70, we could detect expression on activated $CD4^+$ and $CD8^+$ T cells from healthy controls and heterozygous parents, but this mAb did not readily detect expression from P3 and P4 (Fig. 2, C and D; and not depicted). In contrast, the same patients' cells showed normal levels of CD70 proteins by Western blotting using a polyclonal antibody encompassing and extending upstream from the C terminus (Ab3; Fig. 1 E and Fig. 2 E). Next, we tested whether the mutation altered the structure of CD70 sufficiently to impair receptor–ligand interactions. Besides altered epitope binding by Abs, we found no binding of soluble recombinant CD27-Fc to HEK293T cells overexpressing mutant versus WT CD70 (Fig. 2 F). This signal was specific for CD27 as shown by lack of binding to anti-CD5 in WT CD70-transfected cells. The mutant CD70 was expressed to near-equal levels as WT CD70 on trans-

Downloaded from http://rupress.org/jem/article-pdf/214/1/91/1133722/jem_20160849.pdf by Ankara Universitesi Fen user on 11 December 2021

fected cells (Fig. 2, G and H; and not depicted). Together, these data indicate that the mutant CD70 identified in P3 and P4, though expressed, is a loss-of-function variant because of impaired binding to its natural receptor CD27.

Reduced memory B and T cells in CD70-deficient individuals

Although frequencies of B cells and $CD8^+$ T cells were largely normal in CD70-deficient patients, there were mild reductions in proportions of $CD4^+$ T cells (Table 2). Further analysis revealed increased frequencies of naive $CD4^+$ and $CD8^+$ T and B cells and corresponding decreases in memory T cell subsets and total and switched memory B cells (Table 2). Expression of activation and differentiation molecules such as CD27, CD57, CD95, and KLRG1 on memory $CD4^+$ and $CD8^+$ T cells, as well as proportions of regulatory T cells and circulating T follicular helper cells, were comparable between patients and controls (Table 2 and not depicted). In contrast, relative expression levels of 2B4 (CD244) or NKG2D, two activating receptors implicated in $CD8^+$ T cell–mediated control of EBV-infected B cells (Hislop et al., 2010; Palendira et al., 2011; Chaigne-Delalande et al., 2013), were reduced or absent, respectively, on central memory T (T_{CM}; $CCR7^+$ $CD45RA^-$), effector memory T (T_{EM}; $CCR7^-CD45RA^-$), and terminally differentiated effector memory T (T_{EMRA}; $CCR7^-CD45RA^+$) cell subsets of $CD8^+$ T cells from all CD70-deficient patients compared with healthy controls (Fig. 3, A and B). Partial defects in 2B4 and NKG2D expression were also observed for heterozygous carriers (Fig. 3, A and B). Proportions of NK cells and NK subsets in the CD70-deficient patients were variable but largely comparable with healthy controls (Table 2). Thus, although global lymphocyte differentiation in vivo was relatively unaffected by the absence of functional CD70, the maintenance or persistence of memory T and B cells and acquisition of 2B4 and NKG2D by memory $CD8^+$ T cells were compromised.

Altered phenotype of EBV-specific $CD8^+$ T cells in CD70-deficient individuals

Next, we investigated whether EBV-specific $CD8^+$ T cells were present in the CD70-deficient individuals. PBMCs from P1 and P2 (family 1; both HLA-A*24^+) and HLA-matched and -mismatched controls were stained ex vivo with HLA-A*2402–RYSIFFDY tetramers (EBNA3A, residues 246–253). Comparable frequencies of EBV-specific $CD8^+$ T cells were identified in CD70-deficient individuals, heterozygous family members, and healthy HLA-matched controls (0.2–0.5% of $CD8^+$ T cells; Fig. 3 C). The proportions of EBV-specific $CD8^+$ T cells detected in P3 and P4 (family 2; both HLA-A*11^+) using an HLA-A*1101–AVFDRKSDAK tetramer (EBNA3B, residues 399–408) approximated those in HLA-mismatched controls (~0.2% vs. 0.5–1.0% of $CD8^+$ T cells in healthy HLA-matched controls and heterozygous family members), suggesting a negligible EBV-specific response in these individuals (Fig. 3 C). Next, we determined the differentiation status of EBV-specific $CD8^+$ T cells in family 1. As previously described (Callan et al., 1998; Hislop et al., 2002), most EBV-specific $CD8^+$ T cells in healthy donors are T_{EM} cells, with the remainder corresponding to T_{CM} and T_{EMRA} subsets. Intriguingly, most EBV-specific $CD8^+$ T cells in CD70-deficient individuals exhibited a naive ($CCR7^+CD45RA^+$) or T_{CM} cell–like phenotype. Although EBV-specific T_{EM} cells were detected in these patients, they persisted at lower frequencies than controls (Fig. 3 D). Similar to total memory $CD8^+$ T cells, CD27, CD57, KLRG1, CD95, and PD-1 were expressed to comparable levels on EBV-specific $CD8^+$ T cells from CD70-deficient individuals and controls. Importantly, proportions of EBV-specific $CD8^+$ T cells expressing 2B4 or NKG2D were reduced in the CD70-deficient individuals (Fig. 3 E). Moreover, coexpression patterns differed among CD70-deficient individuals, heterozygous relatives, and controls. Most T cells in P1 did not coexpress any of these markers, whereas T cells from P2 predominantly expressed PD-1 (Fig. 3, F and G). Overall, these results suggested that though there is no indication of T cell exhaustion in CD70 deficiency, the phenotype and function of EBV-specific $CD8^+$ T cells is nonetheless altered, with reduced frequencies of T_{EM} cells and reduced expression of 2B4 and NKG2D.

CD70 deficiency impairs cytotoxicity of $CD8^+$ T cells against EBV–B cell targets

Next, we addressed the consequences of CD70 deficiency on lymphocyte function. Proliferation of $CD4^+$ and $CD8^+$ T cells induced by in vitro stimulation of PBMCs with PHA/IL-2, PMA/ionomycin, or immobilized mAbs specific for CD2, CD3, and CD28 was unaffected by CD70 deficiency (Fig. 4 A). Lysis of K562 or 721.211 target cells by IL-2–stimulated NK cells from CD70-deficient patients was normal (P1 and P2) or only modestly reduced (P3 and P4) compared with those from healthy controls (not depicted). Thus, CD70 deficiency has minimal if any effect on the development, differentiation, and function of human NK cells. However, EBV-specific $CD8^+$ T cells from CD70-deficient patients, expanded by co-culturing with irradiated autologous EBV-transformed B lymphoblastoid cell lines (LCLs), exhibited defective cytotoxic activity against EBV-LCL (Fig. 4 B). To determine at which stage of $CD8^+$ T cell activation and differentiation the CD27–CD70 interaction was critical, we tested the effect of CD70 blockade on responses of T cells or clones from healthy donors to autologous EBV-LCL. Up-regulation of CD25 expression on $CD4^+$ and $CD8^+$ T cells by co-culture with EBV-LCL was reduced in the presence of a blocking anti-CD70 mAb (Fig. 4 C). Although the proportion of $CD8^+$ T cells induced to express NKG2D was not affected by CD70 blockade, its level of expression was significantly reduced (Fig. 4 C). Consistent with these findings, up-regulation of CD25 on T cells from CD70-deficient patients was impaired after a 4-d culture with autologous EBV-LCL cells (Fig. 4 D). In contrast, blocking CD27–CD70 interactions did not affect the cytotoxicity of antigen-specific

Downloaded from http://rupress.org/jem/article-pdf/214/1/91/1133722/jem_20160849.pdf by Ankara Universitesi Fen user on 11 December 2021

$CD8^+$ T cell clones against autologous EBV-LCL presenting specific peptides (Fig. 4 E). Thus, CD27–CD70 interactions are required for the initial priming of antigen-specific T cells but not for their subsequent effector function.

DISCUSSION

We have identified four patients from two unrelated kindreds with autosomal recessive CD70 deficiency. Their clinical and immunological features bear similarities to CD27-deficient patients (Table 3). Both groups are prone to hypogammaglobulinemia, EBV-induced disease including lymphoproliferation and lymphoma, and additional viral infections. One of the four CD70-deficient patients had alopecia areata and features of Behçet's syndrome. Interestingly, Behçet's syndrome can be mimicked by EBV-induced uveitis and oral/perianal ulcers, as previously reported for CD27-deficient patients (Alkhairy et al., 2015a). The immunological phenotype of CD27- or CD70-deficient patients includes largely normal counts of T, B, and NK cells but reduced proportions of memory B cells. Although some patients with *CD27* (van Montfrans et al., 2012; Salzer et al., 2013) or *CD70* mutations may generate EBV-specific $CD8^+$ T cells, the nature of the EBV-specific $CD8^+$ T cells was aberrant, indicated by impaired cytotoxic responses to EBV, poor expression of 2B4 and NKG2D (CD70 deficiency), or reduced production of IL-2 (CD27 deficiency; van Montfrans et al., 2012). Likewise, a subset of CD27- or CD70-deficient patients exhibited variably reduced NK cell function. These experiments of nature indicate that CD27 and CD70 serve as each other's essential counter structures.

All CD70-deficient individuals are clinically stable (range in age from 8 to 33 yr), whereas CD27 deficiency showed a high rate of mortality (29%; death reported between 2 and 25 yr of age, mainly related to malignancies and infec-

Table 2. **T, B, and NK cell subsets in CD70-deficient individuals**

Lymphocyte population	Healthy controls	Heterozygous relatives	P1	P2	P3	P4
$CD4^+$ T cells (% of lymphocytes)	51.1 ± 5.2	38.4 ± 4.1	**33.9↓**	47.3	**33.7↓**	**29.8↓**
Percentage of $CD4^+$ T cells						
Naive $CD4^+$ T cells	44.4 ± 3.4	52.7 ± 6.6	**64.3↑**	**62.4↑**	**59.1↑**	**81.4↑**
Stem cell memory	3.1 ± 0.3	1.6 ± 0.5	2.5	**4↑**	**0.28↓**	**0.73↓**
Central memory	28.3 ± 3.4	17.6 ± 5.4	**15.3↓**	**9.8↓**	**20.1↓**	**10.8↓**
Effector memory	20 ± 2.7	25 ± 6	14.8	22.4	**10.7↓**	**5.4↓**
Tfh cells	7 ± 1.1	9.8 ± 7.1	**3.6↓**	**12.5↑**	**23.9↑**	NA
Regulatory T cells	6.1 ± 1.1	5.9 ± 0.5	7.4	6.4	5.8	NA
$CD8^+$ T cells (% of lymphocytes)	22.1 ± 3	14.2 ± 1.3	**31.8↑**	**14.5↓**	**35.6↑**	19.8
Percentage of $CD8^+$ T cells						
Naive $CD8^+$ T cells	27.8 ± 3.4	44.2 ± 4.6	**46.9↑**	**45↑**	**48.4↑**	**53.3↑**
Stem cell memory	2.3 ± 0.5	5.8 ± 2.7	**1.2↓**	2.9	**5↑**	**6.5↑**
Central memory	9.4 ± 1.6	8.7 ± 2.9	**2.1↓**	**3.2↓**	**4.5↓**	**17.1↑**
Effector memory	36.3 ± 2.4	25.6 ± 3.1	**9.8↓**	**17.7↓**	**30.8↓**	**16↓**
T_{EMRA}	23.5 ± 3.8	14.6 ± 3.8	**39.9↑**	29.8	**11.3↓**	**7↓**
B cells (% of lymphocytes)	9.7 ± 1.7	21.8 ± 5	10.7	**2.6↓**	**24.2↑**	NA
Percentage of B cells						
Transitional	4.9 ± 0.5	3.6 ± 1	**10.8↑**	**10.5↑**	**9.2↑**	NA
Naive	68 ± 7	70.2 ± 17.5	**82.1↑**	68	**85↑**	NA
Memory	25.1 ± 6.2	24 ± 17	**6.3↓**	15.5	**4.7↓**	NA
Switched memory (% of memory B cells)	54.3 ± 5.1	44.8 ± 23.8	**27.4↓**	**13↓**	**13.4↓**	NA
NK cells (% of lymphocytes)	5.31 ± 0.6	15.8 ±19.7	4.2	5.2	**2.9↓**	5.1
Percentage of NK cells						
$CD56^{bright}$	93 ± 1	96.1 ± 2.4	**84.5↓**	91	**86.3↓**	97.4
$CD56^{dim}$	6.6 ± 1	3.6 ± 2.2	**14.1↑**	**4.06↓**	**13.7↑**	**2.2↓**
$CD16^+$	76.9 ± 2.4	89.5 ± 5.5	**66.9↓**	**88.5↑**	**84.6↑**	**87.5↑**
$CD27^+$	20.5 ± 2	17.3 ± 4.8	20	23.8	18.8	18.7
$CD57^+$	60.2 ± 2.4	78.8 ± 14.7	55.4	**70.7↑**	**54.9↓**	**75.9↑**
$2B4^+$	97.8 ± 0.4	97.5 ± 2.3	**95.7↓**	97.1	98.8	**96↓**
$CD94^+$	54.2 ± 2.5	80 ± 15.9	**37.7↓**	**66.8↑**	**79.2↑**	**64.6↑**
$KLRG1^+$	39.2 ± 5.8	60.6 ± 20.4	**52.6↑**	**62.7↑**	32	42.6
$NKp30^+$	58.7 ± 5.8	27.8 ± 20	**28.3↓**	**32.7↓**	**36.8↓**	63.9
$NKp44^+$	8.7 ± 3.7	4.4 ± 0.5	7.2	**25.4↑**	4.3	12
$NKp46^+$	31.5 ± 6.1	15 ± 11.3	26.6	26.7	37.5	**45.4↑**

The proportions and phenotype of the indicated lymphocyte subsets were determined as detailed in the B, T, and NK cell phenotyping section of Materials and methods. Subsets of cells were defined as follows: naive ($CD45RA^+CCR7^+CD95^-$), stem cell memory ($CD45RA^+CCR7^+CD95^+$), central memory ($CD45RA^-CCR7^+$), effector memory ($CD45RA^-CCR7^-$), and T_{EMRA} ($CD45RA^+CCR7^-$) $CD4^+$ and $CD8^+$ T cells; regulatory T cells ($CD4^+CD25^{hi}CD127^{lo}$); T follicular cells (Tfh; $CD4^+CD45RA^-CXCR5^+$); transitional ($CD20^+CD10^+CD27^-$), naive ($CD20^+CD10^-CD27^-$), and memory ($CD20^+CD10^-CD27^+$) B cells; and class switched memory B cells ($CD20^+CD10^-CD27^+IgM^-IgD^-$). Values from patients that are above or below two SDs of average value of controls are in bold.

Downloaded from http://rupress.org/jem/article-pdf/214/1/91/1133722/jem_20160849.pdf by Ankara Universitesi Fen user on 11 December 2021

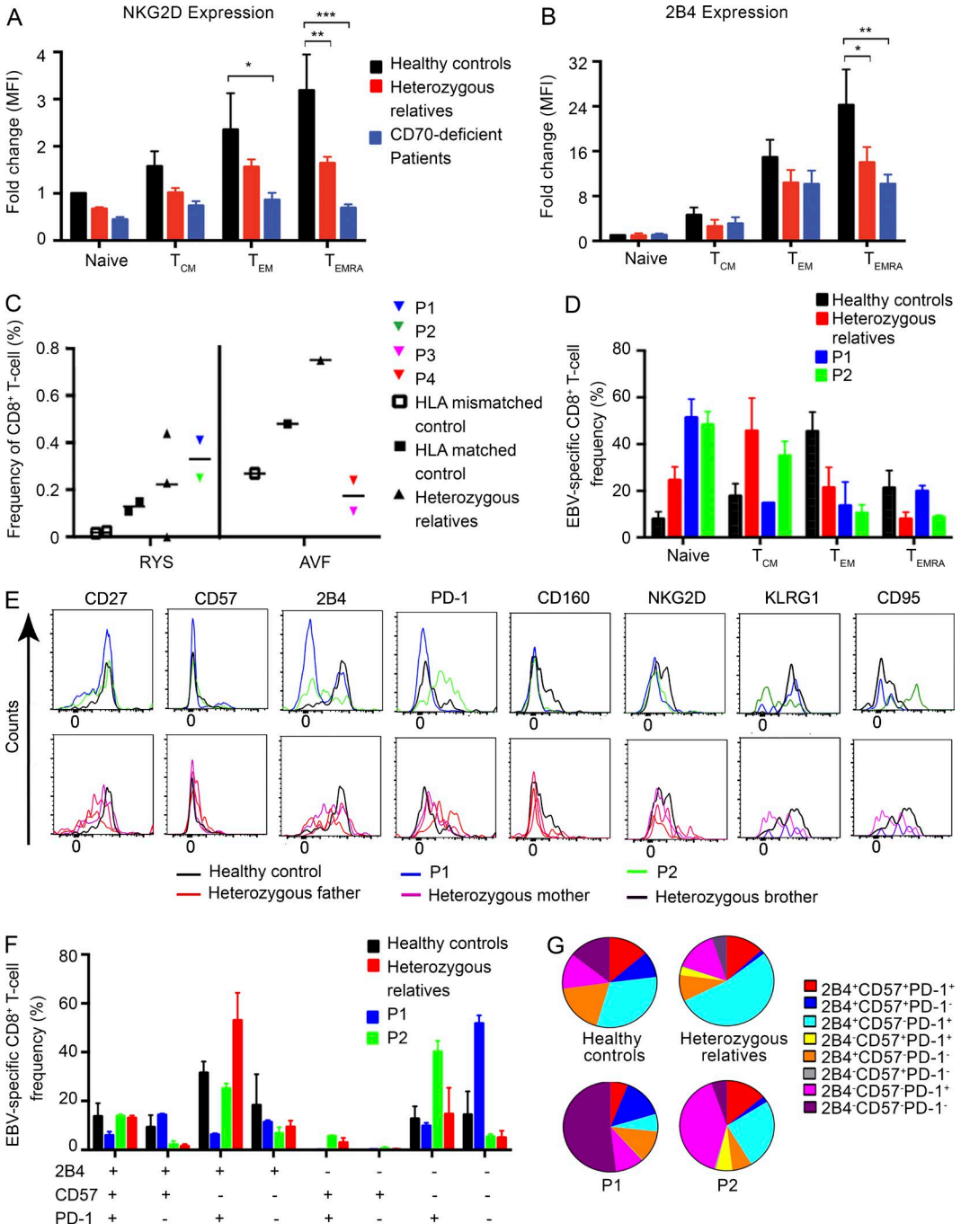

Figure 3. **Phenotype of EBV-specific CD8⁺ T cells in CD70-deficient individuals.** (A and B) PBMCs from healthy donors ($n = 5$), heterozygous carriers ($n = 5$), and CD70-deficient patients ($n = 4$) were labeled with mAbs against CD3, CD8, CD45RA, CCR7, NKG2D, and 2B4. Naive ($CD45RA^+CCR7^+$), T_{CM} ($CD45RA^-CCR7^+$), T_{EM} ($CD45RA^-CCR7^-$), and T_{EMRA} ($CD45RA^+CCR7^-$) $CD8^+$ T cells were identified, and then, expression of NKG2D (A) and 2B4 (B) on each subset was determined. Data are expressed as fold-change in mean fluorescence intensity (MFI; mean ± SEM) relative to expression on naive $CD8^+$ T cells from healthy donors (normalized to 1). The statistics were performed by two-way ANOVA. *, $P < 0.05$; **, $P < 0.01$; ***, $P < 0.001$. (C) Frequency of EBV-specific $CD8^+$ T cells based on staining with the HLA-A*2402–RYSIFFDY (RYS) or HLA-A*1101–AVFDRKSDAK (AVF) tetramer in CD70-deficient individuals ($n = 4$), heterozygous family members ($n = 4$), and HLA-matched ($n = 3$) and -mismatched ($n = 3$) controls. (D) Total frequency of EBV tetramer⁺ $CD8^+$ T cells (HLA-A*2402–RYS) in naive, T_{CM}, T_{EM}, and T_{EMRA} $CD8^+$ T cell populations in P1 and P2, heterozygous family members ($n = 3$), and HLA-matched controls ($n = 3$). Error bars represent mean ± SEM, and experiments for each patient were done on two separate occasions. (E) Expression of CD57, 2B4, PD-1, CD27, CD160, NKG2D, KLRG1, and CD95 on EBV-specific $CD8^+$ T cells from P1 and P2, heterozygous family members ($n = 3$), and healthy controls ($n = 2$). (F and G) Overlays and SPICE chart of coexpression of regulatory markers of CD57, 2B4, and PD-1 in tetramer⁺ $CD8^+$ T cells. (F) Error bars represent mean ± SEM, and experiments for each patient were done on two separate occasions. All data are representative of two individual experiments.

Downloaded from http://rupress.org/jem/article-pdf/214/1/91/1133722/jem_20160849.pdf by Ankara Universitesi Fen user on 11 December 2021

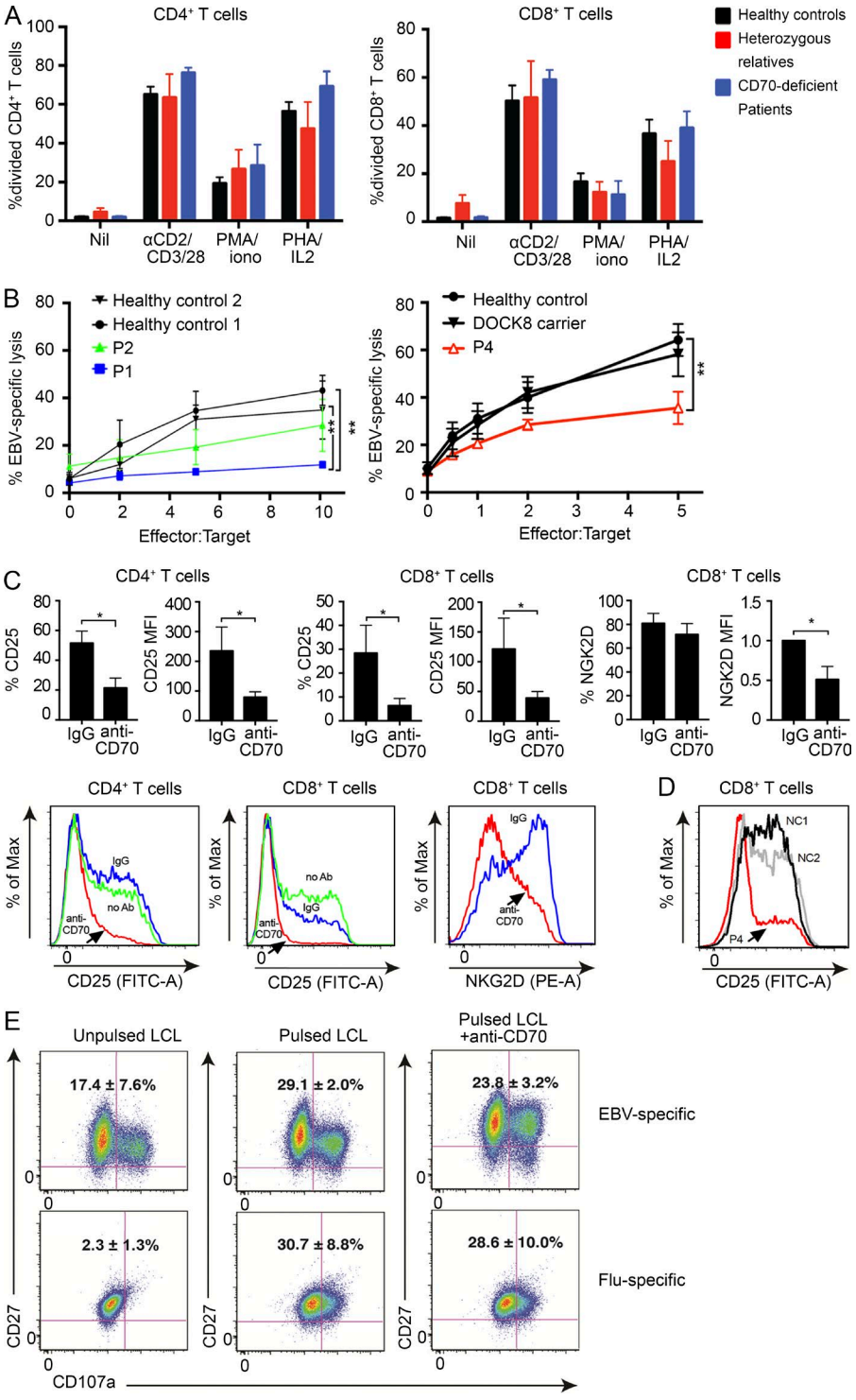

Figure 4. **Impaired cytotoxicity of CD70-deficient CD8⁺ T cells against EBV–B cell targets.** (A) PBMCs from healthy donors (n = 11), heterozygous relatives (n = 3), and CD70-deficient patients (n = 4) were labeled with CFSE and then cultured in vitro in the absence (Nil) or presence of anti-CD2, CD3, CD28 beads, PMA/ionomycin (iono), or PHA/IL-2. Proliferation was determined after 4–5 d by determining the percentage of CD4⁺ or CD8⁺ T cells that had undergone one or more divisions. Values represent the mean ± SEM. (B) Percent lysis of autologous EBV-LCLs by EBV-specific CTL from P1 and P2 (compared with two healthy controls) and P4 (compared with a healthy control and a DOCK8$^{+/-}$ carrier). Shown are means ± SD from two (for P1 and P2) and four (for P4) experiments, respectively. **, $P < 0.005$ by one-way ANOVA. (C) Cell-surface activation marker expression on T cells, induced by EBV-LCLs in the presence of 10 µg/ml anti-CD70 or isotype control. Percent positive or geometric mean fluorescence intensity (MFI) of gated CD4⁺ T cells or CD8⁺ T cells, with CD25 measured at 4 d and NKG2D at 5 d of stimulation is shown. NKG2D mean fluorescence intensity was normalized to that of corresponding isotype control samples. Shown are representative histograms and means ± SD from treatments of PBMCs from four different healthy control donors without prior in vitro stimulation. *, $P < 0.05$ by a Mann-Whitney U test. (D) CD25 induction on T cells from two healthy controls or P4, after 4 d of stimulation by EBV-LCLs. Shown are representative histograms of gated CD8⁺ T cells during the fourth cycle of stimulation with irradiated autologous EBV-LCLs; similar results were obtained during the second or third cycles of stimulation. (E) EBV- or Flu-specific CD8⁺ T cell clones from healthy donors were cultured with autologous EBV-LCLs with or without specific peptides in the absence or presence of 10 µg/ml blocking anti-CD70 mAb. Expression of CD107a by the T cell clones was determined after 6 h. The values represent the mean ± SEM of two or three experiments using EBV-specific or Flu-specific clones, respectively. Note the increased level of activation of EBV-specific CD8⁺ T cell clones in the presence of unpulsed LCLs, over that observed for flu-specific clones, reflects the recognition of peptides by EBV-specific clones presented endogenously (i.e., without pulsing) by the autologous LCLs.

tions; van Montfrans et al., 2012; Salzer et al., 2013; Alkhairy et al., 2015a). It is also notable that the *CD70* heterozygous parents from both families developed cancer, either with an uncommon malignancy (astrocytoma) or at an early age (35 yr), which has not been reported in families of CD27-deficient individuals. Finally, the spectrum of clinical manifestations in CD27- and CD70-deficient individuals varies from asymptomatic to fatal EBV-associated diseases, even among patients carrying the same mutation (van Montfrans et al., 2012; Salzer et al., 2013; this study). It is possible that the con-

Downloaded from http://rupress.org/jem/article-pdf/214/1/91/1133722/jem_20160849.pdf by Ankara Universitesi Fen user on 11 December 2021

text of the primary viral infection—time, location, type, and initial viral load—influences the onset and severity of other clinical/immunological phenotypes. Other genetic modifiers could also interact with environmental factors and, together, account for incomplete penetrance of each viral phenotype and variable expressivity of both conditions.

The CD27–CD70 interaction has been shown to be important for B cell activation, plasma cell generation, and Ig production in vitro (Agematsu et al., 1995, 1999; Jacquot et al., 1997; Borst et al., 2005). Consistent with this notion, all CD70-deficient and 70% of CD27-deficient patients had hypogammaglobulinemia, poor Ab responses to vaccinations, and/or a reduced percentage of switched memory B cells. Nevertheless, it remains unclear whether the antibody defect in CD27 or CD70 deficiency results from defective terminal B cell differentiation and/or lack of T cell help or is caused by EBV or other viral infections. In several CD27-deficient patients, serum Ig levels were normal or high initially but declined dramatically in the months after documented EBV infection. This suggests that hypogammaglobulinemia in these patients may be secondary or facilitated by the underlying genetic defect, as seen in some cases of XLP syndrome (van Montfrans et al., 2012; Salzer et al., 2013; Tangye, 2014).

CD27–CD70 co-stimulation is not critical for T cell development but is involved in peripheral T cell priming and effector functions (Hintzen et al., 1995; Borst et al., 2005). $CD27^{-/-}$ mice show impaired $CD4^+$ and $CD8^+$ T cell priming and T cell memory generation against influenza (Hendriks et al., 2000, 2003). $CD70^{-/-}$ mice have robust cytokine responses during early stages of mouse CMV infection, leading to initial control of viral load; however, they fail to generate an optimal virus-specific cytotoxic T cell response (Allam et al., 2014). The establishment of memory $CD8^+$ T cells and the ability to mount a recall response to LCMV are, however, normal in these mice (Munitic et al., 2013). Furthermore, $CD4^+$ T cell responses are essentially intact in $CD70^{-/-}$ mice (Munitic et al., 2013). IL-2–producing EBV-specific $CD8^+$ T cells were shown to be reduced in one CD27-deficient patient (van Montfrans et al., 2012), whereas EBV-specific $CD8^+$ T cells from CD70-deficient patients exhibited a naive phenotype or were below the limit of detection. Moreover, expression of 2B4 and NKG2D on memory and EBV-specific $CD8^+$ T cells was reduced in CD70-deficient individuals. Impaired signaling through 2B4, a SLAM (signaling lymphocytic activation molecule) family member that recruits SAP (SLAM-associated protein), underlies defective cytolytic responses to EBV infection in SAP-deficient XLP patients (Hislop et al., 2010; Palendira et al., 2011; Waggoner and Kumar, 2012). Similarly, mutations in *MAGT1*, causing X-linked immunodeficiency with magnesium defect, EBV infection, and neoplasia disease, abrogate up-regulation of NKG2D on NK and $CD8^+$ T cells, thereby compromis-

Table 3. **Comparison of the demographic, clinical, and immunological parameters between the four CD70-deficient and 17 reported CD27-deficient patients**

Parameters	CD27 deficiency[a]	CD70 deficiency
Demographic data		
Number of patients (male/female)	17 (6/11)	4 (3/1)
Parental consanguinity (%)	15 (88)	4 (100)
Nonsense mutations (%)	3 (18)	2 (50)
Number of unique mutations reported	6	2
Median age at onset, yr (range)	6 (1–22)	2 (1–5)
Median age at genetic diagnosis, yr (range)	11 (1–32)	17 (3–30)
Postmortem diagnosis (%)	5 (29)	0
Mortality (%)	5 (29)	0
Clinical manifestation		
EBV-positive serology (%)	7/11 (64)	4 (100)
EBV-related lymphoproliferative diseases (%)	7 (41)	3 (75)
EBV-related autoimmunity/inflammation (%)	5 (29)	1 (25)
Central nervous system infections (%)	2 (12)	1 (25)
Other *Herpesviridae* infection (%)	3 (18)	2 (50)
Neoplasia (%)	9 (53)	3 (75)
HL (%)	3 (18)	3 (75)
Immunological phenotype		
Hypogammaglobulinemia (%)	12 (71)	3 (75)
Specific antibody deficiency (%)	5/12 (42)	2 (50)
Reduced total B cells (%)	2 (12)	0
Increased transitional B cells (%)	2/5 (40)	2/3 (67)
Reduced memory B cells (%)	7/8 (88)[b]	2/3 (67)
$CD8^+$ T cell dysfunction (%)	1/1 (100)	4 (100)
Abnormal NK cell counts (%)	2/14 (14)	0
Abnormal NK cell function (%)	4/6 (67)	2 (50)

[a]Data are extracted from van Montfrans et al., 2012; Salzer et al., 2013; and Alkhairy et al., 2015a.
[b]Note that CD27 is a marker for memory B cells, and in CD27-deficient patients, CD27 is not expressed.

Downloaded from http://rupress.org/jem/article-pdf/214/1/91/1133722/jem_20160849.pdf by Ankara Universitesi Fen user on 11 December 2021

ing their ability to lyse EBV-infected target cells (Chaigne-Delalande et al., 2013). As these studies revealed critical roles for 2B4 and NKG2D in cytotoxic lymphocyte-mediated control of EBV infection, impaired expression of these receptors on memory $CD8^+$ T cells in CD70-deficient patients is consistent with the compromised cytotoxic T cell responses against EBV-infected cells that were also observed. These findings provide a mechanistic explanation of how pathogenic mutations in distinct signaling pathways converge to yield a common clinical phenotype. As co-engagement of 2B4 and NKG2D on human NK cells synergize to yield greater cytotoxicity than engagement of either receptor alone (Bryceson et al., 2009; Kwon et al., 2016), it is possible that the combinatorial effect of concomitant signaling via both of these receptors on $CD8^+$ T cells will also be affected by their diminished expression in the absence of CD70. It is highly likely that parallel defects underlie susceptibility to EBV-induced disease in individuals with biallelic mutations in *CD27*.

In conclusion, we have defined a novel PID resulting from CD70 deficiency characterized by increased susceptibility to EBV-induced disease as well as impairments in T and B cell differentiation, culminating in reduced immunological memory. These findings complement the clinical features of CD27 deficiency and underscore the critical function of CD27/CD70 signaling in regulating humoral and cell-mediated immunity in humans, especially for control of EBV. Overexpression of CD70 has been observed in several autoimmune disorders (Han et al., 2016) and various tumors (Jacobs et al., 2015). Immunotherapy targeting the CD27–CD70 axis has therefore been developed and tested in clinical trials (Jacobs et al., 2015). However, frequently occurring deleterious somatic mutations or large deletions in the *CD70* gene have recently been described in diffuse large B cell or Burkitt's lymphomas (Scholtysik et al., 2012; de Miranda et al., 2014). Our discovery and characterization of CD70-deficient individuals provide further insight into the role of CD27/CD70 in autoimmunity and antitumor response and will refine the targeted therapies to the corresponding diseases. In addition, patients receiving Abs blocking CD27–CD70 interaction should be monitored for EBV-induced malignancies.

MATERIALS AND METHODS

Case studies

The proband from the first family (P1) is a female born to Persian consanguineous parents living in Iran. She was admitted to the hospital at the age of 5 yr because of severe chicken pox infection, which led to varicella pneumonia. At the age of 8 yr, she was seen as an outpatient with symptoms suggestive of Behçet's syndrome, including arthralgia of the knee caused by nonerosive oligoarthritis, oral aphthous ulcers, and posterior uveitis. Administration of oral prednisolone improved her condition. At age 9, the patient was hospitalized for immunological evaluation because of recurrent upper respiratory tract infections including otitis media and sinusitis. Hypogammaglobulinemia and poor antibody responses to tetanus and diphtheria vaccinations, but normal T and B lymphocyte counts, were documented. IVIG replacement and prophylactic treatment with antibiotics reduced the frequency and severity of the infectious episodes. Despite regular follow-up, she developed finger clubbing, mild restrictive and obstructive pulmonary function (assessed by spirometry at age 10), alopecia areata (at age 11), peptic ulcer and gastritis, and splenomegaly and lymphadenopathy (at age 17). A diagnosis of mixed cellularity–type HL was made, compatible with stage IIIE,S. Gastric biopsies from an ulcerated lesion in the lesser gastric curve were also taken during this admission, revealing HL-associated lymphohistiocytic infiltration. DNA prepared from a gastric HL biopsy showed a strong EBV^+ signal, as determined by *EBNA1* gene amplification, suggestive of EBV-driven lymphomagenesis. She responded well to four cycles of chemotherapy (doxorubicin, bleomycin, vinblastine, and dacarbazine) and achieved clinical remission. Antibodies (IgG) against EBV (EBNA), CMV, HSV-1, and varicella zoster virus were present at high titers, but no EBV or CMV genes were detected by PCR in the plasma, suggesting remission of the disease. At her most recent clinical follow-up at age 29 yr, her clinical condition was stable on monthly IVIG and prophylactic antimicrobial therapy.

P1 has four siblings, three of whom are healthy. The fourth sibling (P2) had encephalitis during infancy, which led to mental retardation. The encephalitis was likely caused by an undefined central nervous system viral infection, as bacterial infections and other causes of acute encephalopathy were excluded. Normal lymphocyte counts and normal serum Ig levels but low antibody titers against tetanus and diphtheria in spite of vaccination were observed. His antibody (IgG) titers against EBV, CMV, HSV-1, and varicella zoster virus were also high, but no active infections were detected by PCR. At the most recent follow up at age 33 yr, he was intellectually disabled (IQ-based score 64) but did not present with other clinical manifestations. Both maternal and paternal grandparents died from malignancies. The parents have no signs of immunodeficiency, but the father developed prostate cancer at the age of 53 and the mother had uterine cancer (mixed serous-endometrial carcinoma) and astrocytoma at 53 and 60 yr of age, respectively. The mother also had two unexplained miscarriages.

The proband from the second consanguineous family (P3), of Turkish origin, had recurrent otitis media, frequent fever, and diarrhea episodes starting at 1 yr of age. He was 2.5 yr old when he developed diffuse cervical lymphadenopathy. Excisional biopsy revealed mixed cellularity–type HL that was EBV latent membrane protein 1 (LMP1) antigen positive. EBV VCA IgG was positive, and EBV PCR detected 5,726 copies/ml in blood. Reduced Ig levels were detected at the HL diagnosis, but specific antibody responses were present. Peripheral lymphocyte immunophenotyping was normal except for $CD4^+$ T cell lymphopenia that later resolved. Although remission was achieved with two cycles of OPPA (vincristine [Oncovin], procarbazine, prednisone,

Downloaded from http://rupress.org/jem/article-pdf/214/1/91/1133722/jem_20160849.pdf by Ankara Universitesi Fen user on 11 December 2021

and doxorubicin [Adriamycin]) and four cycles of COPP (cyclophosphamide, vincristine [Oncovin], procarbazine, and prednisone), relapse of HL occurred in the same region. Three cycles of ABVD (doxorubicin [Adriamycin], bleomycin, vinblastine, and dacarbazine) and 2,000-cGy radiotherapy resulted in complete remission. Ig levels were still low; thus, IVIG and antimicrobial prophylaxis were started. After 9 yr of an uneventful clinical course, he had elevated EBV PCR copy numbers, which were unresponsive to acyclovir treatment but became negative after two doses of rituximab. He currently remains in complete remission at age 16 years without PCR-detectable EBV or CMV in blood.

P3 has a brother (P4) who was almost 3 yr old when he also developed chronic cervical lymphadenopathy with EBV-associated mixed cellular HL. EBV VCA IgG was positive in blood; EBV was also detected by PCR in his cerebrospinal fluid. He had a history of recurrent upper respiratory infections. Similar to his brother, he had normal lymphocyte immunophenotyping but hypogammaglobulinemia, for which IVIG and antimicrobial prophylaxis were given. Although he entered remission after six cycles of ABVD, relapse of the tumor occurred 2 yr later. Histopathologic examination showed positive EBV LMP1 and CD30 consistent with HL. Six cycles of gemcitabine, vinorelbine, and brentuximab were followed by autologous hematopoietic stem cell transplantation. Although he had an episode of posttransplant EBV flare up, he currently also remains in complete remission, without PCR-detectable EBV or CMV in blood.

Clinical evaluation

Written informed consent was obtained from the patients and their relatives or the healthy normal donors. Approvals for this study were obtained from human research ethics committees at St. Vincent's Hospital and Sydney South West Area Health Service, the ethics committees or the Institutional Review Boards of the Karolinska Institutet, the Tehran University of Medical Sciences, Ankara University, and the National Institute of Allergy and Infectious Diseases, National Institutes of Health. An evaluation sheet was used to summarize demographic information of patients including gender, ethnicity, place and date of birth, medical history including the date of PID diagnosis and record of other diseases, clinical manifestations, relevant laboratory tests, and family history.

Genetic analysis

Genomic DNA was extracted from whole blood using the DNeasy Tissue and Blood kit or from formalin-fixed paraffin-embedded tissue using the GeneRead DNA formalin-fixed paraffin-embedded kit (QIAGEN). WES was performed for P1 and P2 on a HiSeq2000 platform (Illumina), and the process of library preparation, read mapping, and variant analysis has been previously described (Abolhassani et al., 2014; Alkhairy et al., 2015b). For family 2, WGS were performed for P4 (60× mean coverage) and both parents (30× mean coverage) using 300 ng genomic DNA (Broad Institute). Single-nucleotide variant and insertion/deletion calling were performed using the Genome Analysis Toolkit (3.4). Existing databases including 1000 Genome, Exome Aggregation Consortium, National Heart, Lung, and Blood Institute exome variant server, and Greater Middle East Variome were used for filtering based on the population frequency for any given variant for both families. *CD70* has a gene damage index of 1.78 and a mutation significance cut-off of 6.208 (Itan et al., 2015, 2016). The combined annotation-dependent depletion scores (Kircher et al., 2014) for the *CD70* variants identified in the two families are 23.7 and 8.053 (both above the gene-specific mutation significance cut-off) and are thus predicted to be deleterious. WES and WGS data have been deposited in the Database of Genotypes and Phenotypes under accession no. phs001245.v1.p1.

Sanger sequencing was conducted to confirm the presence of the *CD70* mutation in the affected siblings and for carrier detection in family 1. Exon 3 of the *CD70* gene was PCR amplified (forward, 5′-CCTCAGTTTCCCTAAACC TCCA-3′ and reverse, 5′-AAGCTCAATGCCTTCTCT TGTC-3′), and the resulting PCR products were sequenced at Macrogen Inc. Sequence analysis was performed using the Lasergene software package (DNAStar). The same method was applied to investigate the mutation prevalence in this exon in 251 Iranian blood donors. A nested PCR approach was used to amplify *EBNA1* from DNA from tumor biopsy (Cinque et al., 1993; Chan et al., 2001). For variants from family 2, genomic DNA from both affected siblings and parents was PCR amplified (forward primer, 5′-GGCCCCTGT GTGTACACTTT-3′ and reverse primer, 5′-TCTCAGCTT CCACCAAGGTT-3′). Sanger sequencing of purified PCR products was performed by the Genomics Unit of the Rocky Mountain Laboratories Research Technologies Section of the National Institute of Allergy and Infectious Diseases.

RNA isolation and quantitative PCR

PBMCs were isolated from whole blood by a standard method (Hypaque-Ficoll; GE Healthcare). Total RNA was isolated from PBMCs using the RNeasy Mini kit (QIA GEN). cDNA was synthesized by reverse transcription of 0.5 µg of total RNA using a First-strand cDNA synthesis kit (GE Healthcare). Expression level of *CD70* was measured by quantitative PCR (forward, 5′-GTGATCTGCCTCGTG GTGT-3′ and reverse, 5′-CAGCGTCACCTGGATGTGTA-3′) and normalized to *GAPDH*.

Protein expression analysis of the CD70 mutant identified in family 1

Total RNA was extracted from PBMCs from a healthy volunteer, transcribed into cDNA, and used to amplify the coding region of WT CD70 (forward, 5′-TGCGCAGCGGAG GTGA-3′ and reverse, 5′-AGCAGCAGTGGTCAGGGG-3′). The amplified region was ligated into a pcDNA 3.1B mammalian expression vector (Thermo Fisher Scientific). The *CD70* mutation identified in family 1 was generated using

Downloaded from http://rupress.org/jem/article-pdf/214/1/91/1133722/jem_20160849.pdf by Ankara Universitesi Fen user on 11 December 2021

the CHANGE-IT site-directed mutagenesis kit (Affymetrix). HEK293 cells were transfected with 3 µg of the CD70 WT or mutant plasmids or 3 µg of empty pcDNA vector (mock control) using Lipofectamine 2000 (Thermo Fisher Scientific) according to the manufacturer's instructions. 1 µg of a GFP construct was cotransfected to estimate the transfection efficiency. Cells were lysed 48 h after transfection.

Expression of CD70 on B and T cells was evaluated by flow cytometry (anti-CD70, clone 113-16, BioLegend; anti-CD19 BV711, clone SJ25C1, BD; and anti-CD3 FITC, clone HIT3a, BioLegend). T cells were activated with beads coated with anti-CD3, anti-CD28, and anti-CD2 antibodies (Miltenyi Biotec) for 3 d and cultured with 100 U/ml recombinant human IL-2 (rhIL-2) for up to 22 d before analysis. Protein expression in transfected HEK293 cells was analyzed by Western blotting. CD70 expression was detected with two different antibodies: a rabbit polyclonal antibody recognizing amino acids 61–75 of the WT protein (Sigma-Aldrich) and a mouse mAb recognizing amino acids 45–193 (R&D Systems). Successful transfection was monitored by GFP expression (Cell Signaling Technology), and expression of β-actin (Cell Signaling Technology) served as a loading control.

Expression and functional analysis of the CD70 mutant identified in family 2

Endogenous protein expression in proliferating T cells was analyzed by immunoblotting. CD70 expression was detected using a rabbit polyclonal antibody (ab96323) raised against amino acids 129–193 (Abcam). Expression of HSP90 (BD) served as a loading control. Human *CD70* cDNA cloned in the pCMV6 entry vector was purchased from OriGene (no. RC200410). The c.555-557delCTT mutant was generated by site-directed mutagenesis. Full-length CD70 plasmid was PCR amplified using AccuPrime Pfx SuperMix (Invitrogen) with the primer pair containing the CTT deletion (forward, 5′-CACTGATGAGACCTTTGGAGTGCAGTG-3′ and reverse, 5′-CACTGCACTCCAAAGGTCTCATCAGTG-3′). The mutation was confirmed by Sanger sequencing.

HEK293T cells (ATCC) were transfected with 4 µg WT or mutant CD70 plasmids using Turbofect reagent (Thermo Fisher Scientific). 24 h after transfection, cells were washed with PBS, incubated with 10 mM EDTA/PBS to make a single-cell suspension, and resuspended at 0.5×10^6/ml in staining buffer (50 mM sodium phosphate, pH 7.5, 100 mM potassium chloride, 150 mM sodium chloride, 5% glycerol, 0.2% BSA, and 0.04% sodium azide). Cells were preincubated with 6 µg of human IgG (Grifols) for 15 min at 4°C to block nonspecific binding, followed by addition of 1 µg of either biotinylated CD27-µIg (Ancell) or biotinylated anti–human CD5 mAb (PharMingen) for 30 min at 4°C; bound CD27-Fc/mAb was detected with PE-conjugated streptavidin (Ancell). Flow cytometric analysis was performed using FlowJo software (Tree Star). For evaluation of cell surface expression of WT or mutant CD70 in transfected cells, single-cell suspensions were incubated with PE–anti-CD70 (clone 113-16; BioLegend) or anti-flag M2 antibody (Sigma-Aldrich) followed by PE–anti–mouse IgG1 secondary antibody (BioLegend). CD70 expression was also evaluated by immunoblotting as mentioned in the previous paragraph, with the following modifications. Cells were lysed in radioimmunoprecipitation assay lysis buffer (150 mM NaCl, 20 mM Tris-HCl, pH 8, 1 mM EDTA, and 0.05% Nonidet-P40) supplemented with complete protease inhibitor (Roche), with 20 µg of total protein run per lane. CD70 expression was detected using rabbit polyclonal anti-CD70 (C2745; Sigma-Aldrich) or anti-myc (C3956; Sigma-Aldrich) antibodies.

Cell proliferation assay

PBMCs were thawed and resuspended in sterile PBS/0.1% BSA containing CFSE (eBioscience) at a final concentration of 2.5 µM. Cells were incubated at 37°C for 10 min and then washed with five volumes of ice-cold sterile PBS/0.1% BSA and subsequently plated at $\sim 1.8 \times 10^5$ per well in 96-well U-bottom plates containing either RPMI medium/10% FCS alone or 5 µg/ml PHA (Sigma-Aldrich) plus 50 U/ml IL-2 (PeproTech), 20 ng/ml PMA plus ionomycin (Sigma-Aldrich), or T cell activation and expansion beads (one bead to two cells; Miltenyi Biotec) for 4–5 d. Cells were harvested, stained with Zombie aqua fixable viability dye, anti-CD3 Pacific blue, anti-CD8 APC Cy7 (BioLegend), and anti-CD4 BUV395 (BD), fixed, and run on a cell analyzer (LSRII SORP; BD). Data were analyzed using FlowJo software (Tree Star).

B, T, and NK cell phenotyping

PBMCs from healthy controls (n = 5–11), heterozygous carriers (n = 2–5), and homozygous CD70-deficient patients were labeled with mAb against CD3, CD4, CD8, CD20, and CD16/56 to determine the proportions of $CD4^+$ T, $CD8^+$ T, B, and NK cells within the total lymphocyte population. Subsets of these cells were further enumerated by labeling with respective mAbs. The Abs used were: BUV395–anti-CD20, APC–anti-CD10, PECy7–anti-CD27, PE–anti-IgM, PerCP Cy5.5-streptavidin (BD), and biotinylated anti-IgD mAbs (SouthernBiotech) or APC Cy7–anti-CD4, Alexa Fluor 647–anti-CXCR5, PerCP Cy5.5–anti-CD127, PE Cy7–anti-CD25 (BD), and FITC–anti-CD45RA mAbs (BioLegend), anti-CD3 BV421, anti-CD57 FITC, anti-CD94 APC, anti-CD27 BV786, anti-NKp30 PE, anti-NKp44 Alexa Fluor 647, anti-NKp46 (BD), anti-CD56 BV605, anti-CD16 APC Cy7 (BioLegend), anti-2B4 PE, anti–PD-1 biotin, anti-NKG2D PerCP eFluor 710, anti-CD3 biotin, streptavidin-PE Cy7 (eBioscience), anti-KLRG1 APC (Miltenyi Biotec), and anti–NK-T-B antigen (R&D Systems).

The typing for HLA-A, -B, and -C was performed using the low-resolution kits from Olerup SSP. One million PBMCs from CD70-deficient individuals and HLA-matched and -mismatched controls were stained with 20 µg/ml BV421-conjugated tetramer for 20 min at 37°C as previously described (Price et al., 2005). The EBV epitopes used were HLA-A*1101–AVFDRKSDAK (EBNA3B, residues 399–

Downloaded from http://rupress.org/jem/article-pdf/214/1/91/1133722/jem_20160849.pdf by Ankara Universitesi Fen user on 11 December 2021

408) and HLA-A*2402–RYSIFFDY (EBNA3A, residues 246–253). Cells were subsequently stained with APC Cy7–anti-CD8α, PE Cy7–anti-CCR7 (BioLegend), BUV395–anti-CD4, BV605–anti-CD45RA, PE CF594–anti-CD95, BV711-streptavidin, PE–anti-CD160, FITC–anti-CD57 (BD), PE–anti-2B4, PerCP eFluor 710–anti-NKG2D, and biotinylated anti–PD-1 mAbs (eBioscience). Data were acquired on a cell analyzer (LSR II SORP) and analyzed using FlowJo software. Based on Boolean gating analysis, coexpression was determined using SPICE software (Roederer et al., 2011).

Cytotoxic T and NK cell killing assay

For the generation of EBV-transformed LCLs, PBMCs were infected with EBV-containing supernatant from the B95-8 cell line (a gift from J. Cohen, National Institute of Allergy and Infectious Diseases, National Institutes of Health, Bethesda, MD) in RPMI medium containing 20% FBS (Hyclone), 2 mM glutamine, 100 U/ml penicillin and streptomycin (Invitrogen), 55 µM 2-mercaptoethanol (2-ME; Sigma-Aldrich), and 0.2 µg/ml cyclosporine A. Cells were cultured at 37°C for 3–4 wk for emergence of transformed B cells.

EBV-specific CTLs were generated from PBMCs of patients or controls as previously described (Chaigne-Delalande et al., 2013). In brief, PBMCs were cultured in RPMI 1640 medium (Invitrogen) supplemented with 20% FBS (Hyclone), 2 mM glutamine, 100 U/ml penicillin and streptomycin (Invitrogen), and 55 µM 2-ME with 40-Gy γ-irradiated autologous EBV-LCLs, in the presence of 10 ng/ml rhIL-7 (PeproTech) and 10 pg/ml rhIL-12 (R&D Systems; PeproTech). In some cases, PBMCs were first depleted of NK cells by CD56 microbead selection (Miltenyi Biotec). An effector to stimulator ratio of 20:1 or 40:1 was used. After 10 d, 20 U/ml of rhIL-2 (Proleukin) was added to the medium. Repeated stimulations of EBV-specific CTLs were performed every 7–10 d using γ-irradiated autologous EBV-LCL cells at a ratio of 4:1. CTLs after the third restimulation cycle were used in cytotoxicity assays against autologous EBV-LCLs.

NK cells were isolated from PBMCs using $CD56^+$-positive selection (Miltenyi Biotec). Cells were stimulated with 100 U/ml rhIL-2 (Proleukin) in IMDM containing 10% human AB serum (CellGenix), 2 mM glutamine, 100 U/ml penicillin and streptomycin (Invitrogen), and 55 µM 2-ME. NK cells for up to 10 d of culture were used in cytotoxicity assays against either the K562 or 721.221 cell lines.

NK cell and CTL cytotoxicity were measured using the GranToxilux Plus kit (OncoImmunin, Inc.) according to the manufacturer instructions. Target cells were loaded with 1:3,000 or 1:4,000 TFL4 dye for 1–20 min at 37°C, washed twice in PBS, and plated with effector cells. NK cells and CTLs were plated at an effector/target ratio from 0.5:1 to 5:1 and 2:1 to 20:1, respectively, in the presence of the granzyme B substrate. After 1 h of incubation, cytotoxicity was measured using FACSVerse or FAC SCanto flow cytometers (BD).

CD70 blockade of EBV-specific CTL activation

PBMCs from normal healthy donors were cultured with irradiated autologous EBV-LCLs (as described in the Cytotoxic T and NK cell killing assay section). Anti–human CD70 antibody (clone 113-16; BioLegend) or mouse IgG1 isotype control antibody (clone MOPC-21; BioLegend) was added to the culture medium (2.5–10 µg/ml). After 4–5 d of culture, cells were stained with anti–human CD3 (clone HIT3a), CD4 (clone A161A1), CD8 (clone HIT8a), CD25 (clone BC96), and NKG2D (clone 1D11; BioLegend). Cell-surface expression was detected using FACSCanto or Fortessa flow cytometers (BD). $CD8^+$ T cell clones specific for either EBV or influenza were generated from healthy donors as previously described (Palendira et al., 2011), expanded on feeder cells (irradiated allogeneic PBMCs plus autologous EBV-transformed B cell lines presenting specific peptides) for 7–10 d, and then used in cytotoxicity assays. In brief, $CD8^+$ T cell clones were incubated with EBV-LCLs that were either unpulsed or pulsed with 1 µg/ml of specific antigenic peptides in the absence or presence of blocking anti-CD70 mAb. After 6 h, expression of CD107a by the $CD8^+$ T cells was determined.

Statistical analyses

Prism 7 (GraphPad Software) was used with the indicated tests. For comparison of cytotoxicity curves, areas under the curve for each sample in each experiment were used with one-way ANOVA and Dunnett's multiple comparisons.

Online supplemental material

Fig. S1 shows numeration of peripheral blood lymphocyte subsets in the patients. Table S1 shows complementary immunological and virological investigations in patients from family 1.

ACKNOWLEDGMENTS

We would like to thank M. Bartish for generating the CD70-expressing constructs and for help with Western blotting, A. Zaravinos for help with real-time PCR, H. Ham and K. Payne for technical assistance, J. Cohen for reagents, A. Sönnerborg for assisting with the interpretation of serology tests, J. King for help with editing of the manuscript, and the patients and their families for participating in this study.

This study was supported by the Swedish Research Council (grant to L. Hammarström and Q. Pan-Hammarström), the Swedish Cancer Society (grant to Q. Pan-Hammarström), the Swedish Childhood Cancer Foundation (grant to Q. Pan-Hammarström), the Susan and John Freeman Cancer Research Grant from Cancer Council NSW (Australia; grant RG16-11), and the Intramural Research Program of National Institute of Allergy and Infectious Diseases, National Institutes of Health. The laboratory of Human Genetics of Infectious Diseases is supported by grants from Institut National de la Santé et de la Recherche Médicale, University Paris Descartes, the French National Research Agency under the Investments for the Future program (grant n°ANR-10-IAHU-01), the Rockefeller University, and the St. Giles Foundation. D.A. Price is a Wellcome Trust Senior Investigator. S.G. Tangye is a recipient of a Principal Research Fellowship from the National Health and Medical Research Council of Australia (grant 1042925) and a Fulbright Senior Scholarship.

The authors declare no competing financial interests.

Author contributions: H. Abolhassani collected the clinical data and wrote the paper. E.S.J. Edwards, H. Jing, M. Buggert, L. Du, M. Matsuda-Lennikov, R. Romano, R. Caridha, S. Bade, J. Frederiksen, U. Palendira, M.J. Lenardo, and H.C. Su performed the experiments and analyzed and interpreted the data. M. Fang, Y. Zhang, J.J. McElwee,

Downloaded from http://rupress.org/jem/article-pdf/214/1/91/1133722/jem_20160849.pdf by Ankara Universitesi Fen user on 11 December 2021

and B. Boisson analyzed the WES or WGS data. A. Ikinciogullari, S. Haskologlu, S.K. Bal, F. Dogu, N. Tacyildiz, H.F. Matthews, A. Aghamohammadi, and N. Rezaei collected the clinical materials and data. E. Gostick and D.A. Price provided custom reagents. A.C. Karlsson, M.J. Lenardo, J.L. Casanova, and L. Hammarström supervised the research and modified the manuscript. S.G. Tangye, H.C. Su, and Q. Pan-Hammarström designed the experiments, supervised the research, analyzed and interpreted the data, and wrote the paper.

Submitted: 6 June 2016
Revised: 4 October 2016
Accepted: 7 December 2016

REFERENCES

Abolhassani, H., N. Wang, A. Aghamohammadi, N. Rezaei, Y.N. Lee, F. Frugoni, L.D. Notarangelo, Q. Pan-Hammarström, and L. Hammarström. 2014. A hypomorphic recombination-activating gene 1 (RAG1) mutation resulting in a phenotype resembling common variable immunodeficiency. *J. Allergy Clin. Immunol.* 134:1375–1380. http://dx.doi.org/10.1016/j.jaci.2014.04.042

Agematsu, K., T. Kobata, F.C. Yang, T. Nakazawa, K. Fukushima, M. Kitahara, T. Mori, K. Sugita, C. Morimoto, and A. Komiyama. 1995. CD27/CD70 interaction directly drives B cell IgG and IgM synthesis. *Eur. J. Immunol.* 25:2825–2829. http://dx.doi.org/10.1002/eji.1830251017

Agematsu, K., H. Nagumo, Y. Oguchi, T. Nakazawa, K. Fukushima, K. Yasui, S. Ito, T. Kobata, C. Morimoto, and A. Komiyama. 1998. Generation of plasma cells from peripheral blood memory B cells: synergistic effect of interleukin-10 and CD27/CD70 interaction. *Blood.* 91:173–180.

Agematsu, K., S. Hokibara, H. Nagumo, K. Shinozaki, S. Yamada, and A. Komiyama. 1999. Plasma cell generation from B-lymphocytes via CD27/CD70 interaction. *Leuk. Lymphoma.* 35:219–225. http://dx.doi.org/10.3109/10428199909145724

Aguilar, C., and S. Latour. 2015. X-linked inhibitor of apoptosis protein deficiency: more than an X-linked lymphoproliferative syndrome. *J. Clin. Immunol.* 35:331–338. http://dx.doi.org/10.1007/s10875-015-0141-9

Alkhairy, O.K., R. Perez-Becker, G.J. Driessen, H. Abolhassani, J. van Montfrans, S. Borte, S. Choo, N. Wang, K. Tesselaar, M. Fang, et al. 2015a. Novel mutations in TNFRSF7/CD27: Clinical, immunologic, and genetic characterization of human CD27 deficiency. *J. Allergy Clin. Immunol.* 136:703–712.e10. http://dx.doi.org/10.1016/j.jaci.2015.02.022

Alkhairy, O.K., N. Rezaei, R.R. Graham, H. Abolhassani, S. Borte, K. Hultenby, C. Wu, A. Aghamohammadi, D.A. Williams, T.W. Behrens, et al. 2015b. *RAC2* loss-of-function mutation in 2 siblings with characteristics of common variable immunodeficiency. *J. Allergy Clin. Immunol.* 135:1380–1384.e5. http://dx.doi.org/10.1016/j.jaci.2014.10.039

Allam, A., M. Swiecki, W. Vermi, J.D. Ashwell, and M. Colonna. 2014. Dual function of CD70 in viral infection: modulator of early cytokine responses and activator of adaptive responses. *J. Immunol.* 193:871–878. http://dx.doi.org/10.4049/jimmunol.1302429

Borst, J., J. Hendriks, and Y. Xiao. 2005. CD27 and CD70 in T cell and B cell activation. *Curr. Opin. Immunol.* 17:275–281. http://dx.doi.org/10.1016/j.coi.2005.04.004

Bryceson, Y.T., H.G. Ljunggren, and E.O. Long. 2009. Minimal requirement for induction of natural cytotoxicity and intersection of activation signals by inhibitory receptors. *Blood.* 114:2657–2666. http://dx.doi.org/10.1182/blood-2009-01-201632

Callan, M.F., L. Tan, N. Annels, G.S. Ogg, J.D. Wilson, C.A. O'Callaghan, N. Steven, A.J. McMichael, and A.B. Rickinson. 1998. Direct visualization of antigen-specific $CD8^+$ T cells during the primary immune response to Epstein-Barr virus in vivo. *J. Exp. Med.* 187:1395–1402. http://dx.doi.org/10.1084/jem.187.9.1395

Casanova, J.L. 2015a. Human genetic basis of interindividual variability in the course of infection. *Proc. Natl. Acad. Sci. USA.* 112:E7118–E7127. http://dx.doi.org/10.1073/pnas.1521644112

Casanova, J.L. 2015b. Severe infectious diseases of childhood as monogenic inborn errors of immunity. *Proc. Natl. Acad. Sci. USA.* 112:E7128–E7137. http://dx.doi.org/10.1073/pnas.1521651112

Chaigne-Delalande, B., F.Y. Li, G.M. O'Connor, M.J. Lukacs, P. Jiang, L. Zheng, A. Shatzer, M. Biancalana, S. Pittaluga, H.F. Matthews, et al. 2013. Mg2+ regulates cytotoxic functions of NK and CD8 T cells in chronic EBV infection through NKG2D. *Science.* 341:186–191. http://dx.doi.org/10.1126/science.1240094

Chan, P.K., D.P. Chan, K.F. To, M.Y. Yu, J.L. Cheung, and A.F. Cheng. 2001. Evaluation of extraction methods from paraffin wax embedded tissues for PCR amplification of human and viral DNA. *J. Clin. Pathol.* 54:401–403. http://dx.doi.org/10.1136/jcp.54.5.401

Cinque, P., M. Brytting, L. Vago, A. Castagna, C. Parravicini, N. Zanchetta, A. D'Arminio Monforte, B. Wahren, A. Lazzarin, and A. Linde. 1993. Epstein-Barr virus DNA in cerebrospinal fluid from patients with AIDS-related primary lymphoma of the central nervous system. *Lancet.* 342:398–401. http://dx.doi.org/10.1016/0140-6736(93)92814-A

Cohen, J.I. 2015. Primary immunodeficiencies associated with EBV disease. *Curr. Top. Microbiol. Immunol.* 390:241–265.

De Colvenaer, V., S. Taveirne, M. Delforche, M. De Smedt, B. Vandekerckhove, T. Taghon, L. Boon, J. Plum, and G. Leclercq. 2011. CD27-deficient mice show normal NK-cell differentiation but impaired function upon stimulation. *Immunol. Cell Biol.* 89:803–811. http://dx.doi.org/10.1038/icb.2010.171

de Miranda, N.F., K. Georgiou, L. Chen, C. Wu, Z. Gao, A. Zaravinos, S. Lisboa, G. Enblad, M.R. Teixeira, Y. Zeng, et al. 2014. Exome sequencing reveals novel mutation targets in diffuse large B-cell lymphomas derived from Chinese patients. *Blood.* 124:2544–2553. http://dx.doi.org/10.1182/blood-2013-12-546309

Faitelson, Y., and E. Grunebaum. 2014. Hemophagocytic lymphohistiocytosis and primary immune deficiency disorders. *Clin. Immunol.* 155:118–125. http://dx.doi.org/10.1016/j.clim.2014.09.008

Goodwin, R.G., M.R. Alderson, C.A. Smith, R.J. Armitage, T. VandenBos, R. Jerzy, T.W. Tough, M.A. Schoenborn, T. Davis-Smith, K. Hennen, et al. 1993. Molecular and biological characterization of a ligand for CD27 defines a new family of cytokines with homology to tumor necrosis factor. *Cell.* 73:447–456. http://dx.doi.org/10.1016/0092-8674(93)90133-B

Han, B.K., N.J. Olsen, and A. Bottaro. 2016. The CD27–CD70 pathway and pathogenesis of autoimmune disease. *Semin. Arthritis Rheum.* 45:496–501. http://dx.doi.org/10.1016/j.semarthrit.2015.08.001

Hendriks, J., L.A. Gravestein, K. Tesselaar, R.A. van Lier, T.N. Schumacher, and J. Borst. 2000. CD27 is required for generation and long-term maintenance of T cell immunity. *Nat. Immunol.* 1:433–440. http://dx.doi.org/10.1038/80877

Hendriks, J., Y. Xiao, and J. Borst. 2003. CD27 promotes survival of activated T cells and complements CD28 in generation and establishment of the effector T cell pool. *J. Exp. Med.* 198:1369–1380. http://dx.doi.org/10.1084/jem.20030916

Hintzen, R.Q., S.M. Lens, K. Lammers, H. Kuiper, M.P. Beckmann, and R.A. van Lier. 1995. Engagement of CD27 with its ligand CD70 provides a second signal for T cell activation. *J. Immunol.* 154:2612–2623.

Hislop, A.D., N.E. Annels, N.H. Gudgeon, A.M. Leese, and A.B. Rickinson. 2002. Epitope-specific evolution of human $CD8^+$ T cell responses from primary to persistent phases of Epstein-Barr virus infection. *J. Exp. Med.* 195:893–905. http://dx.doi.org/10.1084/jem.20011692

Hislop, A.D., U. Palendira, A.M. Leese, P.D. Arkwright, P.S. Rohrlich, S.G. Tangye, H.B. Gaspar, A.C. Lankester, A. Moretta, and A.B. Rickinson.

Downloaded from http://rupress.org/jem/article-pdf/214/1/91/1133722/jem_20160849.pdf by Ankara Universitesi Fen user on 11 December 2021

2010. Impaired Epstein-Barr virus-specific CD8$^+$ T-cell function in X-linked lymphoproliferative disease is restricted to SLAM family-positive B-cell targets. *Blood*. 116:3249–3257. http://dx.doi.org/10.1182/blood-2009-09-238832

Itan, Y., L. Shang, B. Boisson, E. Patin, A. Bolze, M. Moncada-Vélez, E. Scott, M.J. Ciancanelli, F.G. Lafaille, J.G. Markle, et al. 2015. The human gene damage index as a gene-level approach to prioritizing exome variants. *Proc. Natl. Acad. Sci. USA*. 112:13615–13620. http://dx.doi.org/10.1073/pnas.1518646112

Itan, Y., L. Shang, B. Boisson, M.J. Ciancanelli, J.G. Markle, R. Martinez-Barricarte, E. Scott, I. Shah, P.D. Stenson, J. Gleeson, et al. 2016. The mutation significance cutoff: gene-level thresholds for variant predictions. *Nat. Methods.* 13:109–110. http://dx.doi.org/10.1038/nmeth.3739

Jacobs, J., V. Deschoolmeester, K. Zwaenepoel, C. Rolfo, K. Silence, S. Rottey, F. Lardon, E. Smits, and P. Pauwels. 2015. CD70: An emerging target in cancer immunotherapy. *Pharmacol. Ther.* 155:1–10. http://dx.doi.org/10.1016/j.pharmthera.2015.07.007

Jacquot, S., T. Kobata, S. Iwata, C. Morimoto, and S.F. Schlossman. 1997. CD154/CD40 and CD70/CD27 interactions have different and sequential functions in T cell-dependent B cell responses: enhancement of plasma cell differentiation by CD27 signaling. *J. Immunol.* 159:2652–2657.

Jung, J., J. Choe, L. Li, and Y.S. Choi. 2000. Regulation of CD27 expression in the course of germinal center B cell differentiation: the pivotal role of IL-10. *Eur. J. Immunol.* 30:2437–2443. http://dx.doi.org/10.1002/1521-4141(2000)30:8<2437::AID-IMMU2437>3.0.CO;2-M

Kircher, M., D.M. Witten, P. Jain, B.J. O'Roak, G.M. Cooper, and J. Shendure. 2014. A general framework for estimating the relative pathogenicity of human genetic variants. *Nat. Genet.* 46:310–315. http://dx.doi.org/10.1038/ng.2892

Kwon, H.J., G.E. Choi, S. Ryu, S.J. Kwon, S.C. Kim, C. Booth, K.E. Nichols, and H.S. Kim. 2016. Stepwise phosphorylation of p65 promotes NF-κB activation and NK cell responses during target cell recognition. *Nat. Commun.* 7:11686. http://dx.doi.org/10.1038/ncomms11686

Lens, S.M., R. de Jong, B. Hooibrink, G. Koopman, S.T. Pals, M.H. van Oers, and R.A. van Lier. 1996. Phenotype and function of human B cells expressing CD70 (CD27 ligand). *Eur. J. Immunol.* 26:2964–2971. http://dx.doi.org/10.1002/eji.1830261223

Munitic, I., M. Kuka, A. Allam, J.P. Scoville, and J.D. Ashwell. 2013. CD70 deficiency impairs effector CD8 T cell generation and viral clearance but is dispensable for the recall response to lymphocytic choriomeningitis virus. *J. Immunol.* 190:1169–1179. http://dx.doi.org/10.4049/jimmunol.1202353

Nolte, M.A., R.W. van Olffen, K.P. van Gisbergen, and R.A. van Lier. 2009. Timing and tuning of CD27-CD70 interactions: the impact of signal strength in setting the balance between adaptive responses and immunopathology. *Immunol. Rev.* 229:216–231. http://dx.doi.org/10.1111/j.1600-065X.2009.00774.x

Palendira, U., and A.B. Rickinson. 2015. Primary immunodeficiencies and the control of Epstein-Barr virus infection. *Ann. N.Y. Acad. Sci.* 1356:22–44. http://dx.doi.org/10.1111/nyas.12937

Palendira, U., C. Low, A. Chan, A.D. Hislop, E. Ho, T.G. Phan, E. Deenick, M.C. Cook, D.S. Riminton, S. Choo, et al. 2011. Molecular pathogenesis of EBV susceptibility in XLP as revealed by analysis of female carriers with heterozygous expression of SAP. *PLoS Biol.* 9:e1001187. http://dx.doi.org/10.1371/journal.pbio.1001187

Picard, C., W. Al-Herz, A. Bousfiha, J.L. Casanova, T. Chatila, M.E. Conley, C. Cunningham-Rundles, A. Etzioni, S.M. Holland, C. Klein, et al. 2015. Primary immunodeficiency diseases: an update on the classification from the international union of immunological societies expert committee for primary immunodeficiency 2015. *J. Clin. Immunol.* 35:696–726. http://dx.doi.org/10.1007/s10875-015-0201-1

Price, D.A., J.M. Brenchley, L.E. Ruff, M.R. Betts, B.J. Hill, M. Roederer, R.A. Koup, S.A. Migueles, E. Gostick, L. Wooldridge, et al. 2005. Avidity for antigen shapes clonal dominance in CD8$^+$ T cell populations specific for persistent DNA viruses. *J. Exp. Med.* 202:1349–1361. http://dx.doi.org/10.1084/jem.20051357

Roederer, M., J.L. Nozzi, and M.C. Nason. 2011. SPICE: exploration and analysis of post-cytometric complex multivariate datasets. *Cytometry A.* 79A:167–174. http://dx.doi.org/10.1002/cyto.a.21015

Salzer, E., S. Daschkey, S. Choo, M. Gombert, E. Santos-Valente, S. Ginzel, M. Schwendinger, O.A. Haas, G. Fritsch, W.F. Pickl, et al. 2013. Combined immunodeficiency with life-threatening EBV-associated lymphoproliferative disorder in patients lacking functional CD27. *Haematologica.* 98:473–478. http://dx.doi.org/10.3324/haematol.2012.068791

Scholtysik, R., I. Nagel, M. Kreuz, I. Vater, M. Giefing, C. Schwaenen, S. Wessendorf, L. Trümper, M. Loeffler, R. Siebert, and R. Küppers. 2012. Recurrent deletions of the TNFSF7 and TNFSF9 genes in 19p13.3 in diffuse large B-cell and Burkitt lymphomas. *Int. J. Cancer.* 131:E830–E835. http://dx.doi.org/10.1002/ijc.27416

Scott, E.M., A. Halees, Y. Itan, E.G. Spencer, Y. He, M.A. Azab, S.B. Gabriel, A. Belkadi, B. Boisson, L. Abel, et al. Greater Middle East Variome Consortium. 2016. Characterization of Greater Middle Eastern genetic variation for enhanced disease gene discovery. *Nat. Genet.* 48:1071–1076. http://dx.doi.org/10.1038/ng.3592

Silva, A., D.M. Andrews, A.G. Brooks, M.J. Smyth, and Y. Hayakawa. 2008. Application of CD27 as a marker for distinguishing human NK cell subsets. *Int. Immunol.* 20:625–630. http://dx.doi.org/10.1093/intimm/dxn022

Tangye, S.G. 2014. XLP: clinical features and molecular etiology due to mutations in SH2D1A encoding SAP. *J. Clin. Immunol.* 34:772–779. http://dx.doi.org/10.1007/s10875-014-0083-7

Tangye, S.G., Y.J. Liu, G. Aversa, J.H. Phillips, and J.E. de Vries. 1998. Identification of functional human splenic memory B cells by expression of CD148 and CD27. *J. Exp. Med.* 188:1691–1703. http://dx.doi.org/10.1084/jem.188.9.1691

Taylor, G.S., H.M. Long, J.M. Brooks, A.B. Rickinson, and A.D. Hislop. 2015. The immunology of Epstein-Barr virus–induced disease. *Annu. Rev. Immunol.* 33:787–821. http://dx.doi.org/10.1146/annurev-immunol-032414-112326

Tesselaar, K., L.A. Gravestein, G.M. van Schijndel, J. Borst, and R.A. van Lier. 1997. Characterization of murine CD70, the ligand of the TNF receptor family member CD27. *J. Immunol.* 159:4959–4965.

Tesselaar, K., Y. Xiao, R. Arens, G.M. van Schijndel, D.H. Schuurhuis, R.E. Mebius, J. Borst, and R.A. van Lier. 2003. Expression of the murine CD27 ligand CD70 in vitro and in vivo. *J. Immunol.* 170:33–40. http://dx.doi.org/10.4049/jimmunol.170.1.33

van Montfrans, J.M., A.I. Hoepelman, S. Otto, M. van Gijn, L. van de Corput, R.A. de Weger, L. Monaco-Shawver, P.P. Banerjee, E.A. Sanders, C.M. Jol-van der Zijde, et al. 2012. CD27 deficiency is associated with combined immunodeficiency and persistent symptomatic EBV viremia. *J. Allergy Clin. Immunol.* 129:787–793.e6. http://dx.doi.org/10.1016/j.jaci.2011.11.013

Vossen, M.T., M. Matmati, K.M. Hertoghs, P.A. Baars, M.R. Gent, G. Leclercq, J. Hamann, T.W. Kuijpers, and R.A. van Lier. 2008. CD27 defines phenotypically and functionally different human NK cell subsets. *J. Immunol.* 180:3739–3745. http://dx.doi.org/10.4049/jimmunol.180.6.3739

Waggoner, S.N., and V. Kumar. 2012. Evolving role of 2B4/CD244 in T and NK cell responses during virus infection. *Front. Immunol.* 3:377. http://dx.doi.org/10.3389/fimmu.2012.00377

Downloaded from http://rupress.org/jem/article-pdf/214/1/91/1133722/jem_20160849.pdf by Ankara Universitesi Fen user on 11 December 2021